Mon. Not. R. Astron. Soc. **000**, 000–000 (0000) Printed 23 January 1996 (MN LaTeX style file v1.3)

# Blue compact dwarf galaxies and new velocities in Virgo

M. J. Drinkwater[1], M. J. Currie[2], C. K.Young[3], E. Hardy[4,5] and J. M. Yearsley[6]

[1] *Anglo-Australian Observatory, Coonabarabran, New South Wales 2357, Australia*
[2] *Rutherford Appleton Laboratory, Chilton, Didcot, Oxfordshire OX11 0QX*
[3] *Department of Physics, University of Oxford, Nuclear and Astrophysics Laboratory, Keble Road, Oxford OX1 3RH*
[4] *Département de Physique, Observatoire du Mont Mégantic, Université Laval, Québec, Québec G1K 7P4, Canada*
[5] *Observatorio Astronomico Nacional, Universidad de Chile, Casilla 36-D, Santiago, Chile*
[6] *School of Mathematics and Physical Sciences, University of Sussex, Brighton BN1 9QH*

Accepted 1995 October 17. Received 1995 August 1; in original form 1994 October 24

## ABSTRACT

We present new spectral observations of 303 galaxies brighter than $B_J = 17.6$ in the central 30 square degrees of the Virgo cluster field. The galaxies were selected from two overlapping samples designed for a search for blue compact dwarf (BCD) galaxies and for a more general study of Virgo dwarf-elliptical (dE) galaxies. Many of these galaxies were designated 'background' (i.e. not members of the Virgo cluster) on morphological grounds by Binggeli, Sandage, & Tammann in their *Virgo Cluster Catalog* (VCC). Our principal aim was to measure radial velocities of these galaxies in order to determine which were members of the cluster, looking in particular for any cluster members previously misclassified as background galaxies.

We measured reliable velocities for 291 galaxies, of which 9 were found to be cluster members. Five of these were listed in the VCC as 'members' and 4 as 'possible members'. We also confirmed that 10 VCC 'background' galaxies were correctly identified, and determined that an additional 3 VCC 'possible members' were background galaxies. These results show that the VCC membership estimates were generally correct.

Our sample of candidate BCD galaxies was defined by objective criteria from digitised plate material and therefore allows us to place new limits on the dwarf-galaxy population. We confirm the drop in the BCD luminosity function at an absolute magnitude of $M_B = -14$ reported by Binggeli, Sandage, & Tammann (using their Virgo distance modulus). We also show that if BCDs fade at the end of the current burst of star formation, such 'dead' BCDs, if they exist, would have to all be fainter than our sample limit of $B_J = 17.6$. We use a $(U - B_J)(B_J - R_F)$ colour-colour diagram plotted from our photographic data to separate the different dwarf-galaxy types effectively and use this colour information to argue that there are no blue star-forming progenitors of dE galaxies in the cluster.

Most of the galaxies of compact appearance we selected were background objects which we show are significantly younger than general field galaxies; this sample also shows considerable clustering in redshift space.

**Key words:** galaxies: clusters: general – galaxies: clusters: individual: Virgo – galaxies: distances and redshifts – galaxies: formation.

## 1 INTRODUCTION

The Virgo cluster has long been used as our best laboratory in which to study the formation and evolution of dwarf galaxies (e.g. Binggeli, Sandage, & Tammann, 1985a) because of its proximity and size. The absence of any other galaxies immediately behind the cluster, (in this paper we define the Virgo cluster as the galaxies between us and this void) means that it is mostly, but not always, easy to determine if a given galaxy is in the cluster or not purely on morphological grounds as did Binggeli, Sandage, & Tammann (1985b) in compiling the *Virgo Cluster Catalog* (VCC). There are limitations to this approach however: it fails to account for the line-of-sight depth or structure (Fukugita, Okamura & Yasuda, 1993; Young & Currie, 1995); about 25 per cent of VCC galaxies have uncertain ('possible member') designations and it is also likely that some very high- or very low-surface brightness galaxies have been missed.

In the VCC Binggeli, Sandage, & Tammann listed some 2096 galaxies. They classified about 1277 galaxies as cluster members on morphological grounds, although only 572 had measured radial velocities. In a recent compilation, Binggeli, Popescu & Tammann (1993) presented new velocities for 144 VCC galaxies. There are still many more VCC galaxies without velocity measurements and Binggeli et al. (1993) noted that many galaxies classified as 'background' in the VCC may turn out to be cluster members once velocities are available. It is partly to address this problem that we have made the observations described in this paper.

The lack of velocity information that might be used to confirm membership status is a major problem in estimating the luminosity functions of the dwarf populations within the cluster. Two of us (Young and Currie, in preparation) have compiled a three-band ($U, B_J, R_C$) photographic photometry catalogue of galaxies in the direction of the Virgo cluster's core (herein after VPC for *Virgo Photometry Catalogue*). Some initial findings based on the VPC are presented in Young & Currie (1994) in which distance estimates are derived for a sample of Virgo dwarf ellipticals (dEs) but the main catalogue will be published later. Most galaxies listed in the VPC do not have known radial velocities and a resolution of the cluster-membership problem for at least a significant sub-sample of the catalogue is an important stage of this work. Velocity data are also needed for a kinematic analysis of the cluster to determine whether it is a single cluster elongated along the line of sight or comprises groups either side of a main cluster. We intend to address these topics further in subsequent papers.

A specific topic that we address in this paper is the nature of the blue compact dwarf (BCD) galaxies in the Virgo cluster. The evolutionary relationship (if any) between the early type dE dwarfs and the bluer late-type Im and BCD dwarf galaxies is not clear even in such well-studied regions as the Virgo cluster. Binggeli & Sandage (1984) discussed possible relationships between the dE and Im dwarf types, but were unable to reach definite conclusions. They did suggest that BCDs were the same as Ims but seen during a brief burst of star formation. Subsequent work measuring the surface photometry of representative samples of the dwarf galaxies (Bothun et al. 1986) has shown that this scenario is unlikely because both the dEs and BCDs have significantly smaller scale lengths than the Im dwarfs. If the Im dwarfs faded they would not resemble the dEs, although some BCDs could fade to form dEs. In a similar study (Drinkwater & Hardy 1991) we showed that the most compact BCDs could not fade to become like any known cluster dEs because they were too small.

A serious problem in this discussion is the fact that statistical inferences about the different dwarf-galaxy scenarios are being drawn from samples that may be very incomplete. For instance, in the VCC it was noted that some blue compact dwarf (BCD) galaxies were originally misclassified as background galaxies, so the true number of BCDs in the cluster is uncertain. This prompted three of us (Drinkwater, Yearsley and Hardy) to make a search for compact-galaxy candidates (not already classified as cluster members in the VCC) in the direction of the central part of the cluster. Our new sample of BCD candidates differs from those in previous work in that it was selected automatically according to objective criteria from digitised plate-scan data. Velocity measurements are presented in this paper for most, but not all, of these BCD candidates.

The two projects described above motivated independent proposals to use the FLAIR-II multi-object fibre spectrograph of the UK Schmidt Telescope to obtain radial velocities of several hundred galaxies in the central field of the Virgo cluster. Since a significant number of galaxies were common to both projects we combined the observing sessions to maximise the number of galaxies observed. In this paper we present the observational results for 303 galaxies: 232 were BCD candidates, 120 were for the VPC distance scale and luminosity function project and 49 objects were common to both. We present the results of our BCD study in this paper; the VPC sample is discussed by Young & Currie (1995, and subsequent papers in preparation).

In Section 2 we describe the photographic data and how the galaxies were selected, and in Section 3 we describe the FLAIR-II spectrograph and our observations. The velocity measurements are described in Section 4 and a full list of the galaxies is given in the Appendix. Most of the galaxies for which velocities were obtained turned out to be background objects as expected, and in Section 6 we describe the implications of these measurements for the different galaxy-formation models and estimates of the Virgo BCD luminosity function. In Section 7 we describe the background galaxies. We summarise our conclusions in Section 8.

## 2 SELECTION OF THE SAMPLES

The region of sky under investigation covered almost an entire UK Schmidt-plate field centred on the Virgo cluster's core (the B1950 co-ordinates of the plate's centre being $12^{\mathrm{h}}27^{\mathrm{m}}$, $+13°30'$). The constraints on the positioning of fibres near to the edges of the FLAIR-II plate holder (fewer degrees of freedom) make it difficult to maintain a uniform sample right to the edge of the field. We therefore limited our field to a square region about $5\overset{\circ}{.}5$ across, with opposite corners at $12^{\mathrm{h}}37^{\mathrm{m}}20^{\mathrm{s}}$, $+16°07'30''$and $12^{\mathrm{h}}14^{\mathrm{m}}39^{\mathrm{s}}$, $+10°36'40''$(B1950). A magnitude limit of $B_J \lesssim 17.6$ was imposed so that most redshifts could be measured in a single night of FLAIR-II observations. Within these limits we selected objects from the following two samples.

### 2.1 The VPC Sample

The general dwarf-galaxy sample was extracted from the *Virgo Photometry Catalogue* of Young & Currie (in preparation, but see also Section 3 of Young & Currie (1995) for preliminary details). The VPC was prepared from digitised scans of four Schmidt plates of the central 23 square-degree region of the Virgo cluster, and contains data for 1180 galaxies brighter than $B_{J_{25}} = 19.0$. The plates were scanned in 'mapping mode' by the COSMOS measuring machine of the Royal Observatory, Edinburgh. We reduced the scans using our own software to divide the light between overlapping images and to yield radial profiles. Although, brightward of $B_{J_{25}} = 16.5$ most of the galaxies in the survey had published velocities, for objects in the isophotal magnitude range $16.5 < B_{J_{25}} \leq 17.0$, published velocities were only available for less than 30 per cent of VPC objects. This fraction dropped to about 10 per cent for $17.0 < B_{J_{25}} \leq 17.5$

**Table 1.** UK Schmidt Plates used for the samples. J4882 did not feature in the BCD sample.

| plate | emulsion | filter | date | exp. (min) | seeing ($''$) |
|---|---|---|---|---|---|
| U9362 | IIIaJ | UG1 | 1984 June 3 | 180 | 2.7 |
| J4882 | IIIaJ | GG395 | 1979 March 23 | 60 | 3.0 |
| J9229 | IIIaJ | GG395 | 1984 April 26 | 60 | 1.7 |
| R4891 | IIIaF | RG630 | 1979 March 26 | 90 | 3.3 |

and less than 0.5 per cent for $17.5 < B_{J_{25}} \leq 18.0$. As there were doubts as to whether FLAIR-II was sensitive enough to yield velocities for the lower-surface-brightness VPC galaxies, the brightest VPC objects without published velocities were targeted preferentially. Due to bad weather, many of the lower surface brightness dE candidates were not observed. We plan further observations to measure the velocities of a sample of lower surface brightness objects, with a view to investigating the kinematics of dEs within the Virgo cluster.

### 2.2 The BCD Sample

The BCD sample was designed to detect new compact galaxies not present or confirmed in the original VCC compilation as hypothesised by Drinkwater & Hardy (1991). To make our selection as objective as possible we based our search on digitised Schmidt plate material measured by the Automatic Plate Measuring (APM) facility at Cambridge. We based our image catalogue on a $B_J$ plate of the Virgo field which was scanned by the APM to record image parameters (positions, magnitudes, classifications, areas, peak intensities and image profiles) for all images to a limit of $B_J = 21.5$ (although we did not go so faint in this study). We matched these data to scans of the corresponding $U$ and $R_F$ plates to give a two-colour data set. The plates used are listed in Table 1.

The APM image intensity measurements were processed to convert them to values linearly related to true magnitude by the APMCAL internal calibration method (Bunclark & Irwin 1983). This calibration is only strictly valid for stellar images, but is sufficient for the compact galaxies we are interested in this work, as was shown in the comparison with the VPC. We defined the zero point of the $B_J$ calibration using the VPC as a reference. For a sample of 212 galaxies that appeared in both the APM and VPC data we found an r.m.s. scatter of 0.2 magnitudes in the fit, indicating that the APM magnitude scale is a reasonable approximation for the compact galaxies in this sample. A problem does arise when the APM image-analysis software fails to resolve two or more very close images, but identifies them as a single detection which we denote as a 'merged' object. In the case of a galaxy merged with a star, the merged object may be classified as a galaxy, but the magnitude estimate would be too bright.

We calibrated the APM $U$ and $R_F$ magnitudes using photoelectric $UBVR$ photometry of 16 galaxies in the field. These data were obtained from Caldwell (1983; 10 galaxies), Meurer (private communication; 4 galaxies) and observations we made on the ANU 40-inch telescope (2 galaxies). We have neglected the small colour term in $U$; the other

**Table 2.** Selection of the BCD candidate sample

| property | limits |
|---|---|
| Field centre | $12^h25^m59^s$, $+13°22'08''$ (B1950) |
| Dimensions | $5\overset{\circ}{.}44 \times 5\overset{\circ}{.}51$ |
| Survey Area | 30.02 deg$^2$ |
| Classification | 'galaxy' or 'merged' |
| Magnitude | $15.70 \leq B_J \leq 17.55$ |
| Parent Galaxy Sample | 665 |
| | |
| Peak intensity | $<$19.8 $B_J$ mag arcsec$^{-2}$ |
| Eccentricity | 0–0.8 |
| Compactness criterion | $\log(\mathrm{area}) < 8.19 - 0.30B_J$ |
| Minimum area (red objects) | $\log(\mathrm{area}) > 10.15 - 0.43B_J$, $(B_J - R_F) > 1.1$ |
| Initial BCD Candidate Sample | 306 |
| | |
| Slit spectroscopy | remove stars |
| Final BCD Candidate Sample | 302 |

Note: image area is measured in units of 1 pixel = 0.29 square arcsec.

colour terms we used are: $B_J = B - 0.28(B - V)$ (Blair & Gilmore 1982) and $R_F = R_C - 0.06(B - R_C)$ (Shanks et al. 1984). All the analysis of the BCD sample was made using magnitudes measured in the system of the photographic bands from the APM data, but in the list of all galaxies in Table 9 we have quoted the VPC $B_J$ magnitude where possible because these are more reliable: the VPC reductions allowed for merged images, and also used a much larger number of calibrators.

As a preliminary to defining the compact galaxy sample we defined a 'parent' or field galaxy sample from the APM $B_J$ plate data. The selection criteria for this sample are listed in Table 2 and basically include the area limits described above and a slightly more conservative magnitude limit of $B_J < 17.55$, to increase the fraction of the redshifts that could be measured in a single night. To include as many compact galaxies as possible we selected objects classified by the APM as both 'galaxies' and 'merged'. The merged objects were included because several of the known BCDs were merged, either because of a nearby star or the compact star-forming region itself. The APM photometry of merged galaxies was not corrected for stellar contamination. We note that the astrometry of merged objects is degraded to an uncertainty of typically 5–10 arcsec compared to about 2 arcsec for other galaxies, although this is still accurate enough for this project since we are not limited by confusion. The initial 'parent' sample defined by these criteria consisted of 665 galaxies.

We selected our compact sample using the morphological limits summarised in Table 2. After the magnitude limit and field constraints described above, the most important limit imposed was to put upper limits on the area of an image as a function of magnitude. This is illustrated by the plot of image area against magnitude in Fig. 1 for the parent sample of galaxies and merged objects. Diagrams like this are used in the APM image-classification algorithms to separate stars and galaxies. In this diagram objects with the smallest area at a given magnitude are the most compact and the stellar objects lie in a well-defined locus at the bottom of the diagram. The stellar locus is just visible in Fig. 1

because many of the 'merged' objects we have included are dominated by one or more stars.

Our compact sample was selected by taking all objects below the solid sloping line in Fig. 1. The line was chosen to select compact objects mostly not in the VCC as well as some of the known BCD galaxies which are also indicated in the figure. There is a second line in the figure, drawn to mark off the stellar locus. Many of the objects below this line were found to be dominated by stars, and all the *red* ($B_J - R_F > 1.1$) objects below this line were found to be stars merged with stars and were excluded. Apart from this we did not make any selection by colour. We neither excluded any cases of a star merged with a visible galaxy, nor any stars with no visible diffraction spikes on the $B_J$ plate. This was taken in seeing of 1.7 arcsec, equivalent to about 0.13 kpc in the Virgo cluster so there is a very unlikely that any real galaxies were excluded in this fashion, especially since all the objects considered had image diameters of 12 arcsec or more. Fig. 1 also shows all the 190 VCC galaxies in this region: these are much more extended in size than our compact sample, most being larger than 20 arcsec in diameter.

The initial sample consisted of 306 candidate compact dwarf galaxies. This is listed in the Appendix in Table 9 along with additional galaxies observed for the dE project. Four members of this sample were subsequently revealed to consist of background (non-compact) galaxies merged with stars and were removed to give a final sample of 302 compact galaxies. The colour-magnitude diagram for the compact sample is shown in Fig. 2 with the location of known Virgo dwarf galaxies indicated. Although there is a large dispersion in colour, it is clear that the compact sample is both fainter and bluer in ($B_J - R_F$) colour than the known Virgo dwarfs, most of which are dE types. These colour distributions are discussed further in Section 6.2 below.

## 3 OBSERVATIONS

Our observations were made using the UK Schmidt FLAIR-II multi-object spectrograph during a total of 3 observing seasons from 1992 March to 1994 April. Full details of the spectrograph system are given by Watson et al. (1993); but briefly, it consists of a floor-mounted spectrograph linked by optical fibres to a special-purpose plate holder at the focus of the telescope. This arrangement is ideal for large-area galaxy surveys such as the present projects because up to 92 fibres are available over a field of almost 6°×6°. We observed at the lowest spectral dispersion available using the 250B grating to give a dispersion of 6.1Å per pixel and a resolution of 11Å. The spectral range was 3800–7300Å, although the sensitivity of the system below 4000Å was quite poor.

The dates and other details of our observations are given in Table 3 and all of the galaxies observed and for which we were able to measure radial velocities are listed in Table 9. The co-ordinates in the tables are taken from the APM data and are generally reliable to 2 arcsec except in the case of 'merged' objects (see Section 2.2). The $B_J$ magnitudes in the tables are taken from the VPC where available (i.e. where there is a VPC number quoted in Table 9); otherwise they are are given by the APM data scaled to the same magnitude scale as described in Section 2.2.

**Table 3.** Details of observations

| Run | Date | $T$ (s) | $S$ ($''$) | $B_J$ (mag.) | $\Delta v$ (km s$^{-1}$) |
|---|---|---|---|---|---|
| 1 | 1992 March 2 | 27000$^c$ | 2.5 | 16.0–17.0 | 8 |
| 1a | 1992 March 5 | 15000$^c$ | 2.5 | 16.0–17.0 | 8 |
| 2 | 1992 March 6 | 15000 | 1.5 | 16.0–17.2 | 8 |
| 3 | 1992 March 7 | 18000$^c$ | 2.0 | 16.0–17.2 | 7 |
| 4 | 1993 March 26 | 12000$^c$ | 4.0 | 17.0–17.4 | −2 |
| 5 | 1994 March 12,16 | 13000$^c$ | 3.5 | 16.7–17.4 | −11 |

Notes: $T$ is the total exposure time in seconds ($^c$ indicates cloud-affected exposures); $S$ is the estimated seeing in arcsec; $\Delta v = v_{helio} - v_{obs}$ is the correction applied to the observed velocities to give heliocentric velocities. Most objects from 1992 March 2 were repeated on 1992 March 5 giving a total exposure of 27000s ('Run 1'), except for 8 objects for which strong emission lines were evident in the first night of data. These were not repeated, allowing an additional objects to be observed on the second night only ('Run 1a'), of which 5 yielded velocity measurements.

In a few cases we suspected that the FLAIR-II spectrum of a merged object was contaminated by light from a Galactic star, so these objects were re-observed with a slit-spectrograph on the Anglo-Australian Telescope (service observations by R. Stathakis) and the Australian National University 2.3-m Telescope (observations kindly made by J. Bell).

## 4 VELOCITY MEASUREMENTS

All of our data were processed using the IRAF⋆ image analysis software to obtain one-dimensional, wavelength-calibrated spectra. The spectra were not flux-calibrated: this is difficult to do with the system and is unnecessary for radial velocity measurements. Examples of two spectra are shown in Fig. 3.

The spectra were analysed using the IRAF 'add-on' package RVSAO (Kurtz et al. 1991) to measure their radial velocities. These results are given in Table 9 where the velocities are approximated by $cz$. We obtained reliable velocities for 291 of the 303 galaxies observed using a combination of emission-line fitting and cross-correlation of the spectra with star and galaxy template spectra kindly provided by Dr. Q. Parker. In cases when velocities from both methods were obtained for the same galaxy, we used the measurement with the lower error—usually the emission line velocity. The method of the velocity measurement is indicated by the column labelled 'R' in Table 9. If this is a real number it gives the Tonry & Davis (1979) $R$ coefficient for the cross-correlation peak; we adopted a value of 3.0 as a minimum for acceptance of the result. Note that a small number of measurements passed this test although the line identifications were not convincing on visual inspection.

⋆ IRAF is distributed by the National Optical Astronomy Observatories, which are operated by the Association of Universities for Research in Astronomy, Inc. (AURA) under cooperative agreement with the National Science Foundation.

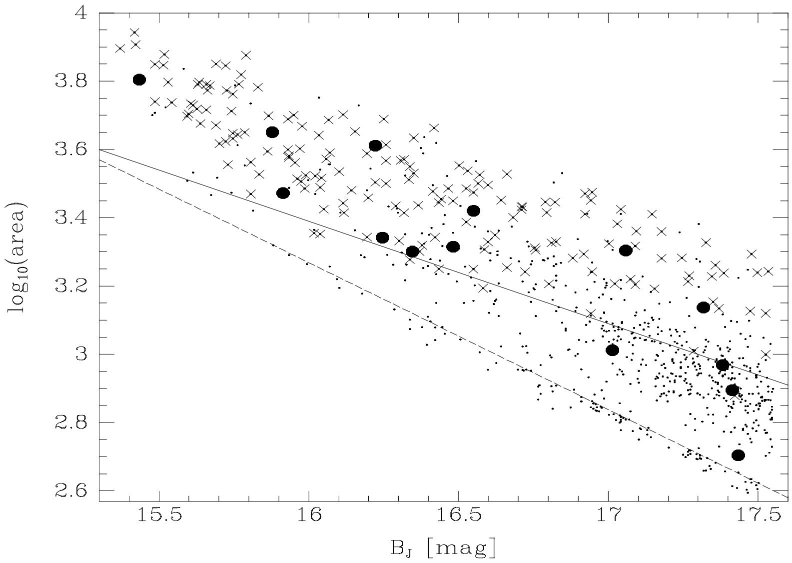


**Figure 1.** An image-classification diagram for galaxies and 'merged' objects in the central region of the Virgo cluster. Each dot represents one object measured on the $B_J$ plate, parameterised by area (in units of 1 pixel ≈ 0.29 square arcsec) and isophotal $B_J$ magnitude. The compact galaxy sample is drawn from objects lying below the solid line; objects lying below the lower line are mostly 'merged' objects dominated by a foreground star and were excluded from the compact galaxy sample. Known BCDs (filled circles) and other galaxies listed in the VCC (crosses) are also indicated.

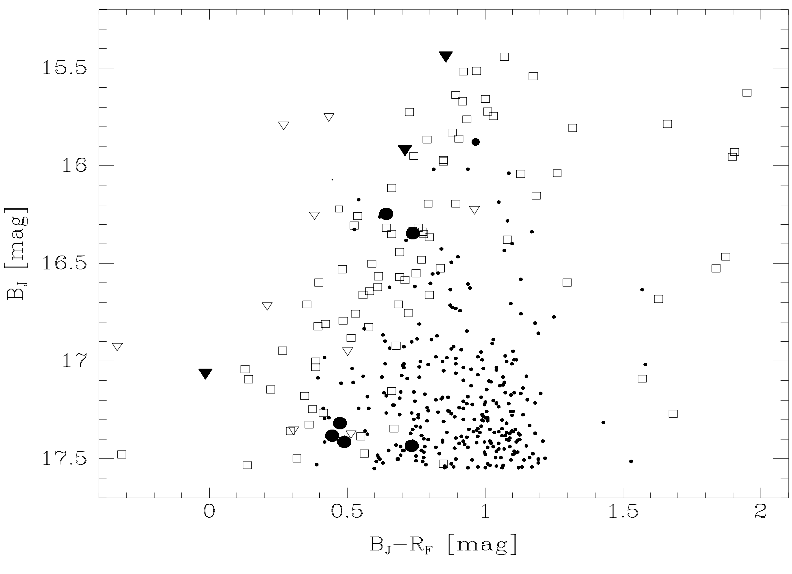


**Figure 2.** Colour-magnitude diagram for the compact galaxy sample (small dots). The large symbols represent dwarf galaxies listed as cluster members in VCC: dE or dE,N (squares) Im (triangles), Im/BCD (filled triangles) and BCD (filled circles).

These galaxies were not included in the 291 reliable measurements, but the results are included in the table with the flag '?' in the final column. If the 'R' value is an integer the redshift was obtained by fitting that many emission lines. If only one line is indicated, this was H$\alpha$. Our sample of measured velocities is incomplete above velocities of about 32000 km s$^{-1}$ corresponding to the point at which the H$\alpha$ line passes out of our observed spectral range. For Runs 1–4 we only used cross-correlation templates with absorption features, whereas in the analysis of Run 5 we used additional templates with emission features. Consequently, a larger proportion of the redshifts in Run 5 were derived from the cross-correlations.

The velocities were corrected from observed to heliocentric values using the corrections quoted in Table 3. The velocity errors given in Table 9 are formal errors from the algorithms used and underestimate the true errors as systematic effects are ignored. Note that the velocities listed in the table are approximations given by $cz$ rather than true velocities.

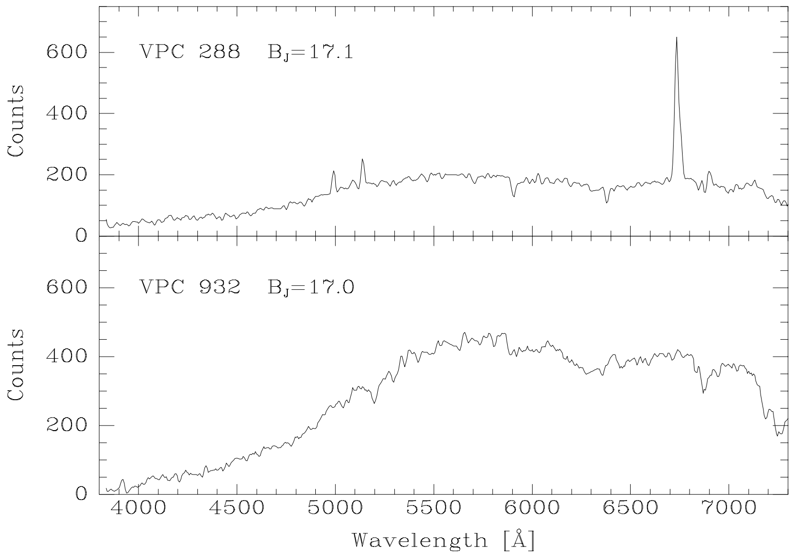


**Figure 3.** FLAIR-II spectra of two of the galaxies observed, one with a velocity fitted by emission lines and one fitted by absorption lines. The spectra have been smoothed on a scale of 3 pixels; the counts are measured in units of electrons per 6Å pixel per 3000-second exposure.

**Table 4.** Velocity Standards

| R.A. (B1950) | Dec. | $B_J$ (mag.) | Name | $v_{\rm helio}$ (km s$^{-1}$) | Ref. |
|---|---|---|---|---|---|
| 12:17:43.0 | 13:41:42 | 17.2 | Bo100 | 24564 | KK2 |
| 12:19:33.6 | 12:01:54 | 15.6 | IC3209 | 7521 | RC3 |
| 12:23:56.9 | 12:26:25 | 16.7 | Bo129 | 16333 | KK2 |
| 12:24:01.1 | 13:01:11 | 16.2 | VCC0916 | 1349 | RC3 |
| 12:28:43.9 | 12:36:27 | 16.2 | VCC1348 | 2272 | RC3 |
| 12:30:00.5 | 14:00:22 | 16.8 | BB391 | 16615 | KK1 |
| 12:30:38.2 | 11:37:22 | 15.9 | IC3483 | 108 | RC3 |
| 12:30:42.0 | 12:31:21 | 15.6 | IC3489 | 7833 | RC3 |
| 12:32:00.3 | 13:46:44 | 15.9 | IC3520 | 1093 | RC3 |

Notes: The galactocentric velocities from KK1 (Karachentsev & Karachentseva 1982) and KK2 (Karachentsev, Karachentseva & Börngen 1983) were corrected to heliocentric values and from RC3 (de Vaucouleurs et al. 1991) we used the optical heliocentric velocities.

In order to estimate the true errors in our velocity measurements we observed a few galaxies of known velocity each night. These are listed in Table 4 along with the heliocentric velocities that we adopted for each. We corrected the published galactocentric velocities in the Karachentsev et al. (1982, 1983) papers to heliocentric values using a velocity vector for the Sun of 232.3 km s$^{-1}$ towards $l$=87°.8, $b$=1°.7 (de Vaucouleurs et al. 1991). The standards are on average somewhat brighter than our programme galaxies, but we note that the faintest gave similar results to the others.

We made a total of 18 measurements of objects with published velocities, and the mean difference between our measured velocities and the standard values ($v_{obs} - v_{std}$) was $-(37 \pm 25)$ km s$^{-1}$. This indicates that there was no significant systematic error in our measurements. The r.m.s. variation in the residuals was $\sigma_v = 106$ km s$^{-1}$. The minimum uncertainty is therefore about $\pm 100$ km s$^{-1}$ and, for a given galaxy, the larger of this value and the formal error given in Table 9 should be used as the uncertainty.

We also reduced Runs 1 through 3 by an independent route using the STARLINK packages CCDPACK, KAPPA, FIGARO and some bespoke applications. The velocities were derived from cross-correlation with both absorption and emission line-spectra. A comparison with 11 of the standard galaxies gave a mean difference of ($v_{obs} - v_{std}$) was $45 \pm 38$ km s$^{-1}$, and an intercomparison with the velocities presented in Table 9 yielded a mean difference of $17 \pm 15$ km s$^{-1}$ ($\sigma_v = 163$ km s$^{-1}$) in the sense the the STARLINK values were larger. We attribute the larger scatter to the sky-subtraction method.

The r.m.s. variation for a simple sky subtraction using the flat field was approximately 15 per cent. This high value probably arises because of the abutted spectra. Using the IRAF route, residual night-sky lines were removed by interpolation. Using the STARLINK software the sky flux was normalised by the strength of the [O I] line at 5077.4Å, but only this sky line was interpolated across to remove any residual. In some cases the remaining residual lines gave large velocity differences accounting for the bulk of the larger deviation. Inadequate sky subtraction, especially the crossover from neighbouring fibres, does limit the effectiveness of FLAIR-II. We estimate that velocities for at least 30 additional dEs in our sample are achievable if we could apply the technique of Lissandrini, Cristiani & La Franca (1994) and approach 2 per cent accuracy in subtraction instead of the ≈10 per cent we achieved.

## 5 MEMBERSHIP

In the absence of any definitive study of the dynamics of the Virgo cluster and given the uncertainty in the depth of the cluster, we have adopted a working definition of cluster 'members' as all galaxies this side of the void between the

**Table 5.** Additional spectroscopic observations of merged objects

| R.A. (B1950) | Dec. | Tel. | VCC | Type | $v_{\rm helio}$ |
|---|---|---|---|---|---|
| 12:19:07.11 | 15:40:31.7 | N1 | - | star | −69 |
| 12:26:43.70 | 10:41:21.8 | N1 | - | star | −28 |
| 12:28:54.85 | 13:11:32.7 | A | - | star | −15 |
| ” | | A | - | galaxy | 28746 |
| 12:29:28.00 | 13:21:32.6 | A | 1403 | star | −69 |
| ” | | A | 1403 | star | −113 |
| ” | | A | 1403 | galaxy | - |
| 12:31:31.61 | 11:17:24.1 | N2 | - | star | -279 |
| ” | | N2 | - | galaxy | 25894 |

Notes: The data were obtained with the ANU 2.3-m Telescope (N1: 1994 July 04, N2: 1995 February 01) and the Anglo-Australian Telescope (A: 1994 April 17).

Local and the Coma superclusters, i.e. at radial velocities $v_{\rm helio} < 3500\,{\rm km\,s^{-1}}$ . This does not strictly imply membership of the Virgo cluster proper. Using this criterion most of the galaxies we measured velocities for turned out to be background objects.

Our FLAIR-II measurements gave 14 objects with velocities of less than $3500\,{\rm km\,s^{-1}}$ but five of these observations were ambiguous. They appeared on the plates as unresolved cores superimposed on extended emission and their spectra showed absorption features only, at very low redshift. These objects were consistent with either cluster galaxies or background galaxies heavily contaminated by superimposed Galactic stars. Subsequent to the FLAIR-II observations we obtained slit spectra of these objects. The additional spatial resolution confirmed that the low redshifts were due to galactic stars, but in two instances we were able to measure a separate redshift for the extended emission which proved to be a background galaxy. We could not obtain a velocity for the galaxy in the other cases. The re-measured velocities are given in Table 5. These objects dominated by foreground stars were removed from the BCD compact-galaxy sample because the background object would not have been ‘compact’ in the absence of the contaminating stars.

After this correction we were left with 9 confirmed cluster members which are listed in Table 6 along with the velocities measured by FLAIR-II. These were all listed in the VCC as ‘members’ or ‘possible members’. We have confirmed all of these identifications with the new velocity measurements.

We measured velocities of greater than $3500\,{\rm km\,s^{-1}}$ for 13 galaxies that are also listed in the VCC. For 10 of these we confirmed the VCC classification as ‘background’ objects and the others were previously classified as ‘possible members’; they are listed in Table 7. These measurements are all consistent with the VCC membership classifications. Although we have shown here that two ‘possible’ BCD galaxies from the VCC are in fact background objects, the overall result of our new velocities combined with those of Binggeli et al. (1993) is that approximately 50 per cent of the ‘possible members’ are members and 50 per cent are background as originally suggested in the VCC.

**Table 6.** Confirmed member galaxies

| R.A. (B1950) | Dec. | VCC | M | Type | $v_{\rm helio}$ |
|---|---|---|---|---|---|
| 12:22:45.53 | 14:26:57.7 | 790 | M | dE1,N | 573 |
| 12:24:22.77 | 13:50:33.8 | 953 | P | dE5?N? | −503 |
| 12:25:09.98 | 12:21:57.8 | 1035 | P | E4 | 182 |
| 12:26:26.27 | 12:56:11.1 | 1148 | P | E0 | 1443 |
| 12:26:42.98 | 13:15:15.7 | 1173 | M | dE5,N | 2468 |
| 12:27:19.49 | 14:08:38.1 | 1237 | P | ? | −336 |
| 12:30:42.39 | 13:08:00.1 | 1491 | M | dE2,N | 1811 |
| 12:31:20.14 | 13:35:53.5 | 1528 | M | d:E1 | 1623 |
| 12:31:43.23 | 11:20:51.3 | 1549 | M | dE3,N | 1366 |

Notes: M gives the membership class (M for member, P for possible member) for any galaxy that is listed in the VCC. The morphological types come the VCC except those in italics that are from our observations.

**Table 7.** Confirmed background galaxies listed in VCC

| R.A. (B1950) | Dec. | VCC | M | Type | $v_{\rm helio}$ |
|---|---|---|---|---|---|
| 12:16:37.01 | 11:59:14.6 | 325 | P | S0: | 16558 |
| 12:16:45.13 | 12:17:40.3 | 337 | B | S | 7819 |
| 12:16:50.14 | 12:19:07.9 | 347 | B | S0/a | 7605 |
| 12:17:15.27 | 12:41:57.3 | 374 | B | S016 | 17778 |
| 12:17:57.53 | 11:37:04.9 | 420 | B | Sa | 12831 |
| 12:18:21.99 | 11:26:20.5 | 443 | B | Sc(r)I | 20487 |
| 12:19:12.96 | 10:52:22.3 | 500 | B | RSB024 | 7840 |
| 12:20:12.71 | 12:34:15.7 | 580 | P | BCD? | 27499 |
| 12:22:05.08 | 11:06:56.6 | 736 | B | SBa(r) | 7661 |
| 12:27:24.23 | 10:53:28.7 | 1243 | B | Sb(s)I-II | 7338 |
| 12:31:40.48 | 12:05:12.0 | 1544 | P | BCD | 16355 |
| 12:33:09.53 | 11:56:31.7 | 1633 | B | SBb(s)I | 16252 |
| 12:33:51.42 | 13:52:39.9 | 1660 | B | Sbc(s)II | 9092 |

Note: the two galaxies VCC1217 and VCC1790 are also possibly background galaxies but we were unable to confirm their velocities.

## 6 COMPACT GALAXIES IN THE VIRGO CLUSTER

As described above, galaxies that we observed for the dE project will be discussed in later papers. We now consider the sample of candidate BCD galaxies defined in Section 2.2. The sample contained 3 known Virgo BCDs with published velocities that were not reobserved; we observed a subset of the sample and measured reliable velocities for 221 of them. Four of these were shown to be contaminated by stars and were excluded from the sample. The remaining 217 galaxies had velocities greater than $5000\,{\rm km\,s^{-1}}$ and were clearly not members of the cluster, although we note that one of them (VCC1544) was listed in the VCC as a possible member. If the 217 galaxies for which velocities were measured are representative of the unobserved galaxies then we can place an upper limit on the number of cluster members in the whole compact sample (excluding the three known BCDs). At the 99 per cent confidence level, the fact that we found no cluster members in 217 measurements implies that the number of members in the whole sample must be less than 2% or 6 galaxies. We do note however that there is a tendency to a smaller success rate at fainter magnitude: 20% of the sample was unmeasured at a magnitude of $B_J = 17.3$ compared to 50% at $B_J = 17.5$.

The result that we found no new compact cluster members has two important consequences which we discuss in this section. First, we can now put tighter limits on the BCD luminosity function, and second, we can place additional constraints on the history of dwarf-galaxy formation in Virgo.

### 6.1 The BCD Luminosity Function

The BCD luminosity function presented by Binggeli et al. (1985a) for the Virgo cluster was limited by the fact that only about half the 64 BCDs counted were confirmed cluster members due to the lack of velocity data. Furthermore there was no objective assurance of completeness because of the many galaxies denoted as 'background' objects on morphological grounds in the absence of velocity measurements.

Within our objective selection limits we can now measure the numbers of Virgo BCDs with a well-defined completeness limit. The region we studied does not cover the whole area surveyed for the VCC, but still contains 191 VCC galaxies in 30 square degrees to our magnitude limit. Of these galaxies, 33 were classified as 'background', 135 as 'members' and 23 as 'possible members' in the VCC. There are 7 BCDs and 4 intermediate (e.g. Im/BCD) types among the members. There were 3 possible BCDs among the possible cluster members, two of which our velocity data now show are in fact background galaxies. Binggeli et al. (1985b) assumed that 50 per cent of the 'possible' members were true members. We find that 2 out of 3 were not members, but this is too small a sample to draw any conclusions and more recent velocity data (Binggeli et al. 1993) indicate that the 50 per cent estimate was accurate and that no significant number of extra objects was included in the BCD luminosity function estimate.

Our new results can be used to show that for compact galaxies within our magnitude limit Binggeli et al. (1985b) did not underestimate the numbers of BCDs either. In the previous section we found that at most 6 of the compact galaxies were cluster members at the 99 per cent confidence level. If we assume that the fraction of BCDs in this sample is 8 per cent as in the other VCC galaxies listed in the region surveyed we find that less than one BCD could have been missed in the compact sample. Our sample is complete to $B_J = 17.55$ or $B = 17.65$ (using $B_J \approx B - 0.1$ for BCDs in our calibration) corresponding to an absolute magnitude at Virgo of $M_B = -14.05$ if we adopt (for convenience) the distance modulus of $(m - M) = 31.7$ mag (Binggeli et al. 1985a); so we can confirm the drop in the BCD luminosity function measured by Binggeli et al. at this absolute magnitude for compact galaxies. We note that this measurement is affected by the uncertainty in the value of the distance modulus adopted and also by the depth of the cluster which may have a range as large as 10–30 Mpc (e.g. Jacoby et al. 1992).

### 6.2 The Evolution of BCDs

In Drinkwater & Hardy (1991) we plotted a diagram of central surface-brightness against scale length for BCDs, dEs and Im types to show that neither the known BCDs nor the Im galaxies could be the progenitors of most dEs because of the very different scale lengths. In Fig. 4 we plot a similar diagram for the current sample, derived from the APM image parameters of peak intensity and image profile. These were simply scaled so that the BCDs imaged by Drinkwater & Hardy (1991) had similar central surface brightnesses and scale lengths respectively. The estimate works well for scale length, but the surface brightness is severely affected by saturation of the measured photographic density at about 21.7 mag arcsec$^{-2}$. An upper envelope to the sample in this plot is defined by the total-magnitude limit used. The plot is nevertheless very useful because it shows a complete sample rather than just relying on which galaxies had been described in the literature as previously. The plot includes members of the candidate BCD sample that could be cluster members as well as all VCC galaxies in our parent sample that were not classified as giant galaxies in the cluster or as background galaxies.

**Table 8.** Photographic colours of the compact galaxy sample and various VCC dwarf galaxies

| type | N | $\overline{(B_J - R_F)}$ | $\sigma_{b-r}$ | $\overline{(U - B_J)}$ | $\sigma_{u-b}$ |
|---|---|---|---|---|---|
| compact | 302 | 0.90 | 0.22 | −0.17 | 0.22 |
| BCD | 7 | 0.64 | 0.19 | −0.40 | 0.33 |
| Im | 9 | 0.36 | 0.34 | 0.09 | 0.44 |
| dE | 78 | 0.76 | 0.44 | 0.40 | 0.38 |

The figure displays the same trend as before, with scale length increasing from BCD to dE to Im types. The mean scale lengths are $3.6 \pm 0.6, 6.6 \pm 0.2$ and $7.7 \pm 0.8$ arcsec respectively. We can use the larger complete sample presented here to examine our earlier suggestion (Drinkwater & Hardy 1991) that there should be small, redder, low surface-brightness counterparts to the most compact BCDs. If the most compact BCDs to the extreme left of Fig. 4 are undergoing a burst of star formation, where are the non-star forming counterparts or 'faded' BCDs? We have the following possibilities.

(i) They may simply fade beyond the limit ($B_J = 17.55, M_{B_J} = -14.15$) of the survey, i.e. above the dotted line in Fig. 4. The models discussed by Bothun et al. (1986) and Searle, Sargent & Bagnuolo (1973) allow fading by up to 1.5 mag which, as we can see from the figure would be enough to move the compact BCD galaxies beyond our magnitude limit. (Note that this is after we have allowed for saturation of the photographic data: Fig. 4 of Drinkwater & Hardy shows that the surface brightness of the BCDs reaches 21.) This fading scenario is also supported by Pustil'nik et al. (1995) on the basis that the spatial distribution of BCDs is consistent with that of low surface brightness dwarfs, although this is for field galaxies and they do not address the scale sizes. There is a clear case for doing a deeper survey of the Virgo cluster to continue looking for faded BCDs.

(ii) The galaxies might get bigger as a result of differential fading and thus move sideways into the dE region of Fig. 4. This might be permitted by our results as we have not investigated larger galaxies, although it was shown to be very unlikely for the very compact BCDs measured by Drinkwater & Hardy.

(iii) These might be the first BCDs to have formed,

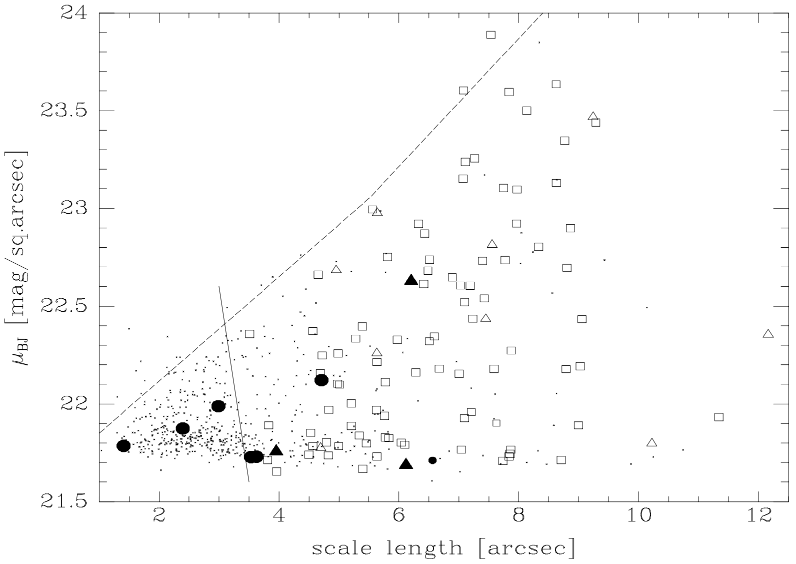


**Figure 4.** Central surface-brightness of galaxies plotted against scale length, both estimated from the APM image parameters. The upper dashed line indicates the magnitude limit ($B_J = 17.55$) of the sample; the lower limit in surface brightness represents saturation at about 21.7 mag; the surface brightness of the most compact galaxies is severely underestimated. The solid line indicates the upper limit in size of the compact sample. The large symbols represent dwarf galaxies listed as cluster members in VCC: dE or dE,N (squares), Im (triangles), Im/BCD (filled triangles) and BCD (filled circles). The small dots represent remaining galaxies in the field sample that are not in the VCC.

so there is no second generation and/or the evolution timescales of BCDs may be longer than previously thought. The fading scenarios are motivated in large by models of star formation in which the blue colours of the Im and BCD dwarfs imply a high rate of star formation which can only be sustained for a short period (Searle et al. 1973), but it has been suggested that the duration constraints may be relaxed in the presence of galactic winds allowing for longer periods of continuous star formation (Meurer, Mackie & Carignan 1994); furthermore, the BCD outer isophotes can be as red as dEs implying a significant population of older stars. Similar conclusions are drawn by James (1994) on the basis of $JHK$ near infra-red photometry of 26 dE, Im and BCD Virgo dwarfs. He finds a clear difference between the young stellar populations of the dIs and older stars in the dEs, as well as dynamical differences, the dEs being much more relaxed dynamically than the Ims. He suggests that the BCDs are an intermediate type, perhaps dEs that have had a recent burst of star formation.

We can estimate the ages of the star-forming populations of these galaxies from models like those of Struck-Marcell & Tinsley (1978) or Kruger et al. (1991) which give loci in the $(U-B)(B-V)$ and $(U-B)(B-R)$ planes respectively as a function of age. We plot the $(U-B_J)(B_J-R_F)$ colour-colour diagram in Fig. 5 for all galaxies in the field sample apart from any classified as giant ellipticals, or spirals, or definite background objects in the VCC. The location of known dwarf-galaxy types from VCC are indicated and the BCD galaxies are seen to be clearly separated from the dEs. The mean colours of the different dwarf types and our compact sample are listed in Table 8. These show the strong signature of star formation in the BCDs which are significantly bluer in $(U-B_J)$ than the dEs. The Im galaxies have a mean $(U-B_J)$ colour intermediate to the dE and BCD types and may be slightly bluer than the BCDs in $(B_J-R_F)$, but the scatter is large, indicative perhaps of the greater uncertainties in the photometry of the more extended Im galaxies.

To estimate ages of the BCDs from this diagram we must chose between burst and continuous star-formation models: we adopt continuous star formation here because of the reddish $(B_J-R_F)$ colours; similar arguments are given for the outer region of NGC1705 by Meurer et al. (1994). The most useful age indicator in our data is the $(U-B_J)$ colour which we note from our calibration data is approximately equal to $(U-B)+0.1$. For a mean $(U-B_J)$ colour of $-0.4$ we get similar ages of about 1 Gyr, although there is quite a spread in measured colours. The bluest BCD galaxies have $(U-B_J)$ as low as $-0.8$ which would imply shorter ages. The errors in the photographic data may be large, but we can confirm at least one of these from our calibration data (BB18 has $U-B_J=-0.78$) and our data imply that RMB132 is also at least this blue, both indicating ages as small as 50 Myr, but these could be explained by the recent formation of a star cluster (Meurer et al. 1994).

### 6.3 Dwarf Elliptical Formation

In a similar fashion we can look for a population of star-forming galaxies with similar scale sizes to the dE galaxies that might be their progenitors. It has already been shown that dwarf irregulars cannot be the progenitors of dEs (Bothun et al. 1986), but that some of the larger BCDs could possibly fade to form smaller dEs (Drinkwater & Hardy 1991). It is hard to see that all the cluster dEs could have formed from BCDs unless we are seeing the cluster at a special time when this formation is just ending. We may have

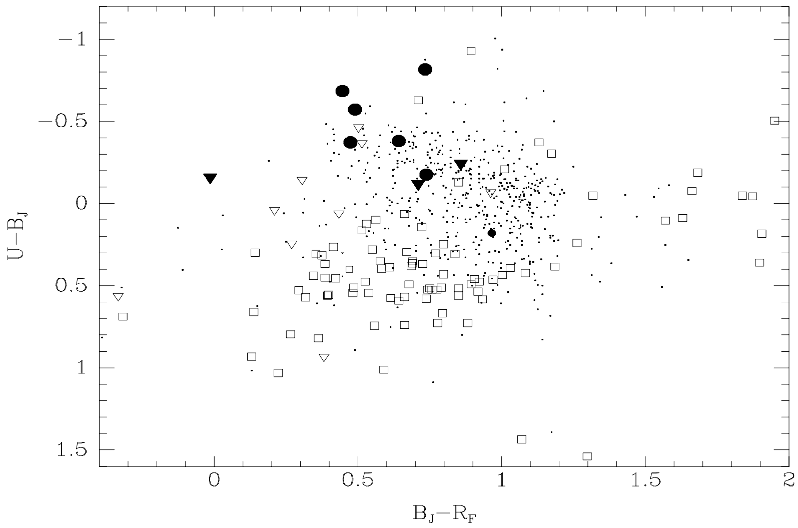


**Figure 5.** Colour-colour diagram of all galaxies in the Virgo sample based on photographic measurements. The symbols represent dwarf types Im (triangles), dE (squares), Im/BCD or Sm/BCD (filled triangles) and BCD (filled circles). The smaller filled circle represents a BCD classified as a possible background galaxy. The small dots represent remaining galaxies in the field sample that are not listed in the VCC.

to consider the possibility that these dwarf galaxy types are not linked in any simple evolutionary path—this is the conclusion that James (1994) reaches based on infrared data.

The region of Fig. 4 most populated by dE galaxies (scales of 4–9 arcsec) was not part of our BCD sample searched for new cluster members, but visual inspection of the galaxies not already listed in VCC from this region showed that most were probably background spirals. A small number (9 in this range) of the uncatalogued galaxies resemble ellipticals and cannot be discounted as possible cluster members. These will form the basis of a future study, although their colours are so red ($\overline{(U-B_J)} = 0.42 \pm 0.05$) that any large amount of star formation is unlikely.

The final word on the origin of the dE types awaits an extension of our spectroscopic survey to larger galaxies, but from Fig. 5 and the above discussion it seems unlikely that a significant fraction were formed through the fading of BCDs. Nor do we find any evidence for any larger star-forming galaxies in the cluster that could be dE progenitors.

## 7 BACKGROUND GALAXIES OF COMPACT APPEARANCE

An interesting result of our search for compact dwarfs in the Virgo cluster is a redshift catalogue of 217 background galaxies selected for compact morphology as opposed to magnitude limit alone as in most galaxy surveys. In this section we discuss the properties of this sample.

### 7.1 Distributions

We intend to produce a detailed analysis of the 3-dimensional distribution to a later paper, therefore we only present a summary of their distributions here. First, in Fig. 6 the distribution of the galaxies as a function of $B_J$ magnitude is given for the two samples. This shows that the BCD candidate sample extends to much fainter total magnitudes, but that is a natural consequence of the fact that these were selected for high central surface brightness.

In Figures 7 and 8 we show velocity histograms for those Virgo galaxies with new redshift measurements, first, all together, and then separated by sample. The BCD candidate sample is seen to extend to larger velocities, again consistent with their selection being biased towards high surface-brightness. There is a peak in the velocities at 7000 km s$^{-1}$ evident in Fig. 7. This is part of the Coma/A1367 Supercluster as discussed previously by Karachentsev (1982), Binggeli et al. (1993), and references therein. The peak at 13000 km s$^{-1}$ could be Supercluster 7 in the Bahcall & Soneira (1984) catalogue.

Fig. 7 shows a non-uniform distribution typical of pencil-beam surveys expected from the bubble-like topology of the large-scale structure. There is some suggestion of periodicity around 50–60$h^{-1}$ Mpc, however, a power-spectrum analysis (Kaiser & Peacock 1991) suggests that is not significant. Our field size is much wider and our redshift depth much shallower than the pencil-beam survey of Broadhurst et al. (1990) that presented evidence that such peaks were periodic with frequency 128$h^{-1}$ Mpc.

### 7.2 Colours and Luminosity Function

It is interesting to compare the properties of the compact sample to those of background field galaxies in general. We define a sample of 'field' galaxies by taking our parent sample of 665 galaxies and removing any listed as members or possible members in the VCC (in the absence of complete velocity information). This leaves a sample of 510 galaxies, of which our compact galaxies are a subsample. We plot

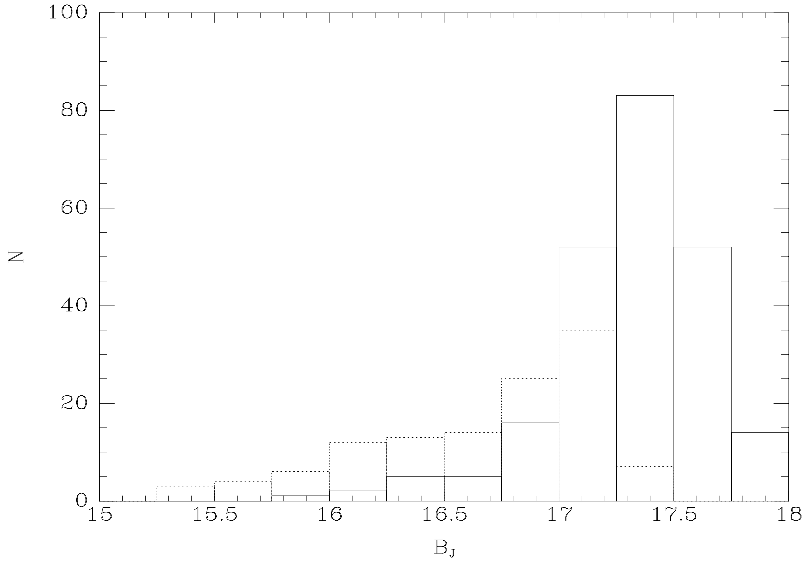


**Figure 6.** Magnitude distribution of the galaxies by type: BCD candidates (solid) and VPC (dotted).

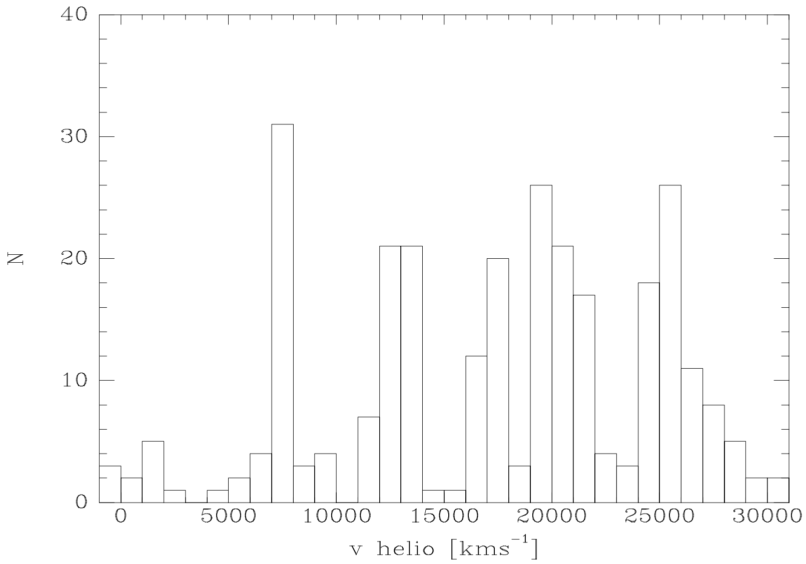


**Figure 7.** Distribution of radial velocities of all galaxies.

the colour distributions of the two samples in Fig. 9 and Fig. 10. We tested for any difference in the distributions using the two-sample Kolmogorov-Smirnov (KS) test. There is no significant difference in the $(B_J - R_F)$ colours (with a probability of 56% of obtaining these values for the same distributions) although there is a tail of very red objects ($B_J - R_F > 1.2$) in the 'field' sample; most of these are galaxies merged with stars in the APM data. We do find that the compact sample is significantly bluer in $(U - B_J)$ than the field sample, with means of $-0.14 \pm 0.01$ and $-0.04 \pm 0.01$ mag respectively and a KS probability of less than 0.01% of getting these from the same distribution. It would therefore appear that by choosing compact galaxies we have selected a younger, more actively star-forming sample than the general population of field galaxies.

We derived the luminosity function for those galaxies in the compact sample with measured velocities using the $\Phi_G$ estimator of Felten (1976), cosmological parameters $H_0 = 50\,\mathrm{km\,s^{-1}\,Mpc^{-1}}$ and $q_0 = 0.5$ and k-corrections based on standard galaxy spectral energy distributions. We used the $(B_J - R_F)$ colours to estimate the galaxy spectral types using the relationships plotted by Colless et al. (1990). We checked the effect of the uncertainty in our colours on the calculation and found it was not significant.

The resulting luminosity function is shown in Fig. 11. We note that because the range in apparent magnitude of our sample was small (mostly 16.5 to 17.5) the luminosity function is affected by the clustering in redshift space apparent in Fig. 7. The figure gives the luminosity function of

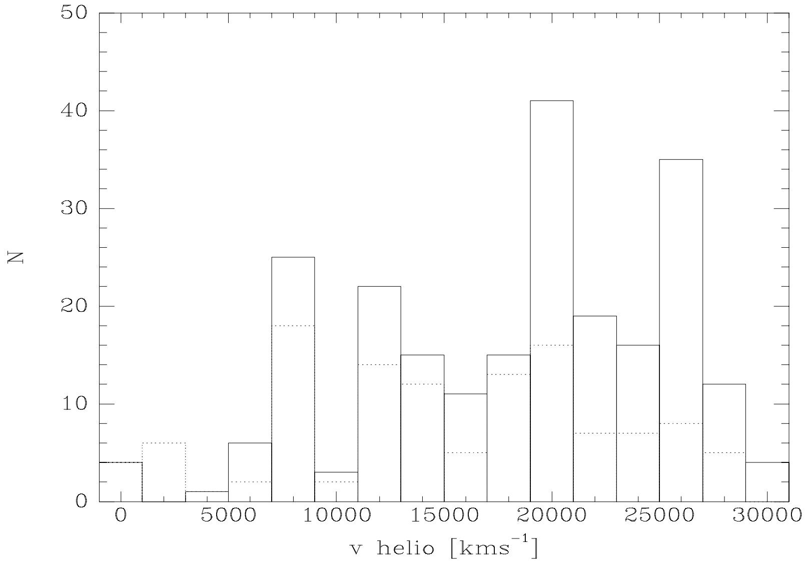


**Figure 8.** Distribution of radial velocities by galaxy type: BCD candidates (solid) and VPC (dotted).

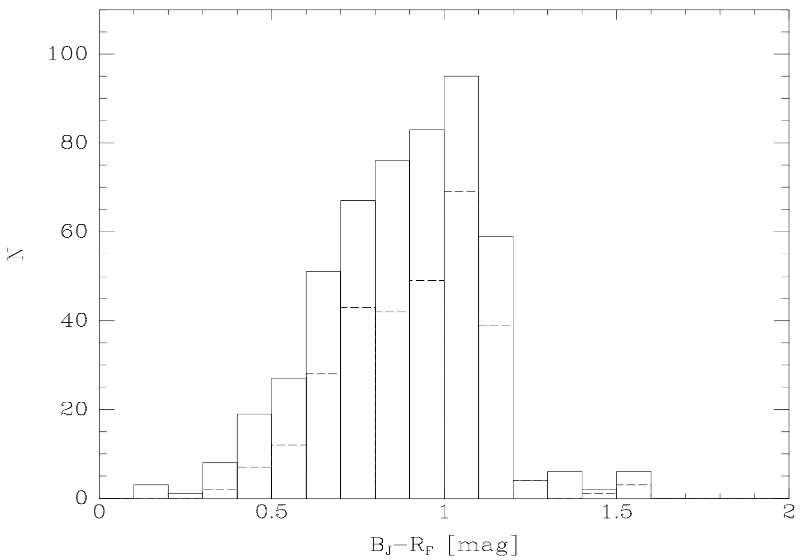


**Figure 9.** $(B_J - R_F)$ colour distribution of background galaxies. The 'field' sample is plotted in solid lines and the compact sample is in dashed lines.

the whole compact galaxy sample, i.e. it is corrected for the fraction of the sample for which redshifts were not measured.

We cannot compare these results directly with the 'field' galaxy sample because the redshifts are not known, but a very useful comparison can be made with results obtained for APM galaxy survey (Loveday et al. 1992). That survey had a similar limiting magnitude to the present sample ($B_J = 17.15$) and was derived from similar digitised plate data. The APM survey luminosity function is also plotted in Fig. 11. It is apparent that the two sets agree for the brighter (more distant) galaxies but that the compact sample contains significantly less fainter (or nearby) galaxies. This is perhaps to be expected from the BCD selection criteria as well as the fact that most VCC galaxies were excluded (the VCC included most galaxies that could possibly be nearby).

## 8 SUMMARY

In this paper we have presented the results of observations of 303 galaxies in the central $5\overset{\circ}{.}5\times5\overset{\circ}{.}5$ field of the Virgo cluster. The aim of the spectroscopic observations was to verify cluster membership for overlapping samples of BCD candidate and VPC galaxies. Of the 291 galaxies for which we obtained reliable velocities, only 9 proved to be definite cluster members. This was to be expected, because very few of the target galaxies were listed in the VCC as members or possible members. We have therefore confirmed with velocity measurements many of the membership classifications made on morphological grounds by Binggeli et al. (1985b). In addition, we have resolved membership uncertainties for 7 of the VCC 'possible' members.

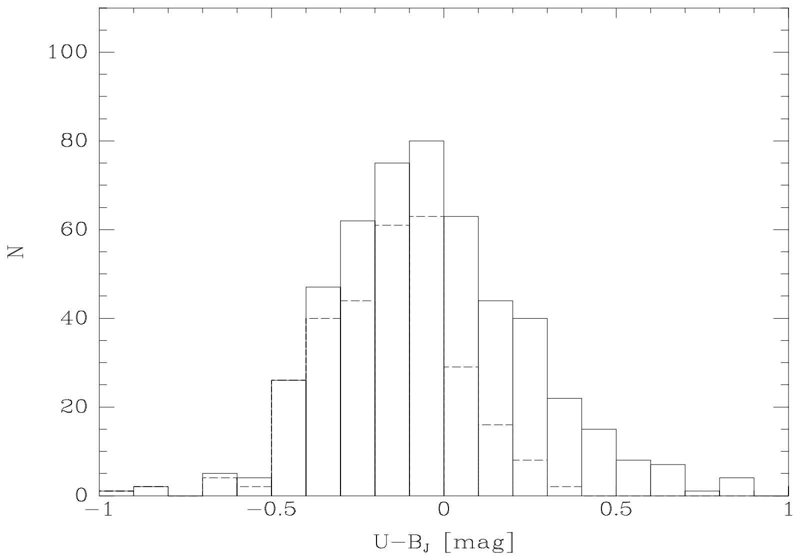


**Figure 10.** ($U - B_J$) colour distribution of background galaxies. The 'field' sample is plotted in solid lines and the compact sample is in dashed lines.

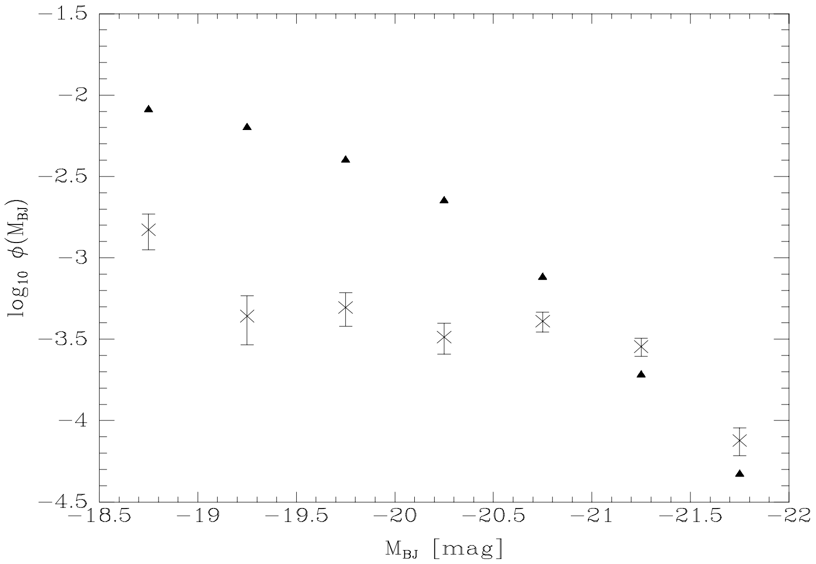


**Figure 11.** Luminosity function of background galaxies. Data from this work are presented as crosses with errors based on Poisson counting statistics and data from the APM galaxy survey (Loveday et al. 1992) are plotted as triangles.

The first of our galaxy samples (for the VPC project) concentrates initially on the cluster's dEs, investigating both their three-dimensional spatial distribution by means of the new distance indicators presented in Young & Currie (1994 & 1995) and their luminosity function. This will be the subject of more detailed analyses to follow in later papers.

Our second galaxy sample (candidate BCDs or compact galaxies) is more complete and has been analysed in this paper. This sample allows us to make several new conclusions about the properties and distribution of compact dwarf galaxies in the Virgo cluster because it was defined by automated selection with objective selection criteria and has well-defined completeness limits.

(i) We confirm the completeness of the BCD luminosity function derived by Binggeli et al. (1985a). In particular, we can confirm the drop in the luminosity function at magnitudes fainter than $B_J$=17.6 ($M_B = -14$ using the Binggeli et al. distance modulus).

(ii) We do not find any evidence of 'red compact dwarf' galaxies that might result from the end of star formation in BCDs within our magnitude and compactness limits. This shows that if star formation in BCDs is short lived, then any in a post-star formation phase must have faded beyond our $B_J = 17.55$ magnitude limit. An alternative suggested by the galaxy colours ($U - B_J$ versus $B_J - R_F$) is that the star formation is slower but longer-lived, removing the need to find 'faded' BCDs.

(iii) Moving to galaxies of larger scale size we have presented evidence that there are no high surface-brightness star forming galaxies in the cluster that could be the progenitors of the main population of dwarf ellipticals. This conclusion needs to be confirmed with additional spectroscopic observations.

Finally we have shown that the background galaxies in the 'compact' sample provide an interesting probe of the large-scale distribution of galaxies. In particular the 'compact' criterion selects selects a population that is significantly younger than general field galaxies and is strongly clustered in redshift space.

## Acknowledgments

We would like to thank Dr. G.R.Meurer for providing additional photometry and Dr. M.M.Colless for providing the software used to calculate the luminosity functions. In addition they both made many helpful suggestions about this paper.

This work has made use of two separate forms of data originating from the UK Schmidt Telescope of the Anglo-Australian Observatory. First, we have analysed Schmidt plates provided by the UK Schmidt Unit, Royal Observatory Edinburgh (ROE). These were digitised by both the APM facility at Cambridge and the COSMOS facility at ROE; specifically we thank Dr. H.M. MacGillivray for dealing with our abnormal requirement. We have also used the FLAIR-II system on the UK Schmidt for spectrographic observations, and we thank Drs. Q.A. Parker and F.G. Watson for all of their assistance at the telescope. We would also like to thank J. Bell for providing additional data from the Australian National University 2.3-m Telescope and R. Stathakis for performing our service observations on the Anglo-Australian Telescope. Dr. F. Valdes has given much helpful advice on the analysis of fibre spectra using the IRAF software, Dr. A. Heavens provided a pre-release version of the improved FIGARO/XCROSS software, Dr. J.A. Peacock calculated the power-spectrum of the velocity distribution and assessed the significance of the main peak, and Dr. B. Binggeli very kindly provided a machine-readable version of the VCC. MJC and CKY thank STARLINK for computing facilities.

This research has made use of the NASA/IPAC Extragalactic Database which is operated by the Jet Propulsion Laboratory, California Institute of Technology, under contract with the National Aeronautics and Space Administration. E.H. has received support from NSERC-Canada, and the 'Fundacion Andes', Chile (C-42944/1).

## REFERENCES

Bahcall. N.A., Soneira R.M., 1984, ApJ, 277, 27
Binggeli, B., Sandage, A., 1984, AJ, 89, 919
Binggeli, B., Sandage, A., Tammann, G.A., 1985a, AnnRevAA, 26, 509
Binggeli, B., Sandage A., Tammann G.A., 1985b, AJ, 90, 1681
Binggeli, B., Popescu, C.C., Tammann, G.A., 1993, AASup, 98, 275
Blair, M., Gilmore, G., 1982, PASP, 94, 742
Bothun, G.D., Mould, J.R., Caldwell, N., MacGillivray, H.T., 1986, AJ, 92, 1007
Broadhurst T.J, Ellis R.S., Koo D.C., Szalay A.S., 1990, Nature, 343, 726
Bunclark, P.S., Irwin, M.J., 1983, in Rolfe, E.J., ed. Statistical methods in Astronomy, European Space Agency SP, vol 201 p. 195
Caldwell, N., 1983, AJ, 88, 804
Colless, M., Ellis, R.S., Taylor, K., Hook, R.N., 1990, MNRAS, 244, 408
Drinkwater, M., Hardy, E., 1991, AJ, 101, 94
Felten, J.E., 1976, ApJ, 207, 700
Fukugita, M, Okamura, S, Yasuda, N., 1993, ApJ, 412, L13
Jacoby, G.H., Branch, D., Clardullo, R., Davies, R.L., Harris, W.E., Pierce, M.J., Pritchet, C.J., Tonry, J.L., Welch, D.L., 1992, PASP, 104, 599
James, P.A., 1994, MNRAS, 269, 176
Kaiser, N., Peacock, J.A., 1991, ApJ, 379, 482
Karachentsev I.D., Karachentseva V.E., 1982, Sov. Astron. Lett., 8(2), 104
Karachentsev I.D., Karachentseva V.E., Börngen F., 1983, Sov. Astron. Lett., 9(4), 205
Karachentsev, I.D., 1982, Sov. Astron. Lett., 8(1), 37
Kruger, H., Fritze von-Alvensleben, U., Loose, H.-H., Fricke, K.J., 1991, AA, 242, 343
Kurtz M.J., Mink D.J., Wyatt W.F., Fabricant D.G., Torres G., Kriss G.A., Tonry J.L., 1991, in Worrall D. M., Biemesderfer C., Barnes J., eds., Astronomical Data Analysis Software and Systems I, ASP Conf. Ser., Vol. 25, p.432
Lissandrini C., Cristiani S., La Franca F., 1994, PASP, 106, 1157
Loveday, J., Peterson, B.A., Efstathiou, G., Maddox, S.J., 1992, ApJ, 390, 338
Meurer, G.R., Mackie, G., Carignan, C., 1994, AJ, 107, 2021
Pustil'nik, S.A., Ugryumov, A,V., Lipovetsky, V.A., Thuan, T.X., Guseva, N,G., 1995, ApJ, 443, 499
Searle, L., Sargent, W.L.W., Bagnuolo, W.G., 1973, ApJ, 179, 427
Shanks, T., Stevenson, P.R.F., Fong, R., MacGillivray, H.T., 1984, MNRAS, 206, 767
Struck-Marcell, C., Tinsley, B.M., 1978, ApJ, 221, 562
Tonry J.L., Davis M., 1979, AJ, 84, 1511
de Vaucouleurs G., de Vaucouleurs A., Corwin H.G., Buta R.J., Paturel G., Fouqué P., 1991, Third Reference Catalogue of Bright Galaxies, Springer-Verlag, New York
Watson F.G., Gray P.M., Oates A.P. & Bedding T.R., 1993, in Wall J.V., ed, Optics in Astronomy, Cambridge Univ. Press, Cambridge, p.49
Young C.K., Currie M.J., 1994, MNRAS, 268, L11
Young C.K., Currie M.J., 1995, MNRAS, 273, 1141

This paper has been produced using the Royal Astronomical Society/Blackwell Science LaTeX style file.

## 9 APPENDIX

We present our combined galaxy sample in Table 9 below. This includes all galaxies from the VPC and BCD samples for which we measured radial velocities plus the additional galaxies making up the complete BCD sample for which velocities were not measured. All the velocities are from our own data except for 6 additional velocities from the literature.

**Table 9.** Combined sample of BCD candidates and other galaxies observed

| N | R.A. (B1950) | Dec. | $B_J$ | B | Y | VPC | VCC | Run | R | $v_{\rm helio}$ | $\sigma_v$ | comment |
|---|---|---|---|---|---|---|---|---|---|---|---|---|
| 1 | 12:14:44.30 | 14:28:38.7 | 17.4 | 1 | 0 | 0 | 0 | - | - | - | - | - |
| 2 | 12:14:55.32 | 13:12:35.0 | 17.3 | 1 | 0 | 0 | 0 | - | - | - | - | - |
| 3 | 12:14:56.64 | 12:54:54.3 | 17.2 | 1 | 0 | 0 | 0 | 1a | 1 | 27780 | 64 | y |
| 4 | 12:15:05.65 | 10:40:05.0 | 17.7 | 1 | 0 | 0 | 0 | 4 | 1 | 25026 | 100 | y |
| 5 | 12:15:36.67 | 11:13:32.9 | 17.1 | 1 | 0 | 0 | 0 | 1 | 4.59 | 7295 | 76 | y |
| 6 | 12:15:38.05 | 13:51:55.8 | 17.5 | 1 | 0 | 0 | 0 | - | - | - | - | - |
| 7 | 12:15:41.70 | 14:56:02.9 | 17.2 | 1 | 0 | 0 | 0 | 1 | 6.11 | 13113 | 51 | y |
| 8 | 12:15:43.57 | 10:56:37.1 | 17.6 | 1 | 0 | 0 | 0 | 5 | 1 | 15644 | 101 | y |
| 9 | 12:15:44.49 | 11:38:46.8 | 17.4 | 1 | 0 | 0 | 0 | 5 | 2.45 | 7817 | 78 | ? |
| 10 | 12:15:44.81 | 13:32:06.4 | 16.6 | 1 | 0 | 0 | 0 | 1 | 2 | 20307 | 79 | y |
| 11 | 12:16:01.60 | 13:07:59.6 | 17.4 | 1 | 0 | 0 | 0 | - | - | - | - | - |
| 12 | 12:16:04.72 | 13:12:54.5 | 16.6 | 1 | 0 | 0 | 298 | - | 0 | 7713 | 0 | (1) |
| 13 | 12:16:10.36 | 11:52:54.9 | 17.5 | 1 | 0 | 0 | 0 | 2 | 3 | 11566 | 44 | y |
| 14 | 12:16:12.70 | 12:10:19.5 | 16.4 | 2 | 0 | 0 | 0 | 4 | 5.25 | 8106 | 56 | y |
| 15 | 12:16:17.58 | 13:10:28.4 | 16.3 | 1 | 1 | 1 | 0 | 1 | 2 | 6023 | 27 | y |
| 16 | 12:16:24.74 | 13:43:50.0 | 17.9 | 1 | 0 | 7 | 0 | - | - | - | - | - |
| 17 | 12:16:27.35 | 12:18:35.4 | 17.6 | 1 | 0 | 11 | 0 | 4 | 3.51 | 7603 | 106 | ? |
| 18 | 12:16:36.09 | 12:14:37.3 | 17.5 | 2 | 0 | 23 | 0 | 5 | 4.07 | 19079 | 65 | y |
| 19 | 12:16:37.01 | 11:59:14.6 | 15.9 | 0 | 1 | 25 | 325 | 1 | 5.38 | 16558 | 63 | y |
| 20 | 12:16:38.44 | 14:48:50.9 | 16.1 | 1 | 1 | 28 | 0 | 1 | 4.73 | 12252 | 74 | y |
| 21 | 12:16:38.87 | 12:16:17.4 | 17.8 | 1 | 0 | 30 | 0 | 2 | 5 | 19359 | 37 | y |
| 22 | 12:16:45.13 | 12:17:40.3 | 16.2 | 0 | 1 | 36 | 337 | 3 | 6.20 | 7819 | 62 | y |
| 23 | 12:16:50.14 | 12:19:07.9 | 16.4 | 2 | 1 | 39 | 347 | 1 | 5.44 | 7605 | 56 | y |
| 24 | 12:16:51.99 | 14:44:53.6 | 17.3 | 2 | 0 | 42 | 0 | 5 | 3.27 | 12072 | 122 | y |
| 25 | 12:16:52.79 | 14:48:29.8 | 16.2 | 1 | 1 | 43 | 0 | 3 | 4.03 | 20929 | 77 | y |
| 26 | 12:16:56.57 | 10:37:03.5 | 17.2 | 2 | 0 | 0 | 0 | 1a | 4.77 | 7143 | 59 | y |
| 27 | 12:16:57.56 | 14:41:06.3 | 17.9 | 1 | 0 | 48 | 0 | 4 | 1 | 21013 | 70 | y |
| 28 | 12:17:01.40 | 12:41:52.9 | 17.1 | 1 | 0 | 50 | 0 | 2 | 3.53 | 17563 | 61 | y |
| 29 | 12:17:03.43 | 13:22:00.5 | 17.8 | 1 | 0 | 52 | 0 | 4 | 3.27 | 28077 | 73 | ? |
| 30 | 12:17:04.45 | 13:44:58.9 | 17.4 | 1 | 0 | 54 | 0 | 5 | 3.91 | 19791 | 105 | y |
| 31 | 12:17:06.34 | 12:16:33.0 | 17.2 | 2 | 0 | 56 | 0 | 2 | 3.76 | 19245 | 100 | y |
| 32 | 12:17:06.76 | 13:45:22.7 | 17.3 | 1 | 1 | 57 | 0 | 1 | 4.85 | 5963 | 67 | y |
| 33 | 12:17:07.09 | 12:40:09.6 | 17.3 | 1 | 0 | 0 | 0 | 4 | 3.53 | 17540 | 83 | y |
| 34 | 12:17:07.44 | 11:20:00.2 | 17.0 | 1 | 0 | 59 | 0 | - | - | - | - | - |
| 35 | 12:17:08.04 | 12:40:58.0 | 17.5 | 2 | 0 | 61 | 0 | 5 | 3.39 | 17695 | 148 | y |
| 36 | 12:17:09.18 | 15:50:33.4 | 17.3 | 1 | 0 | 0 | 0 | - | - | - | - | - |
| 37 | 12:17:10.93 | 13:43:41.4 | 17.1 | 1 | 0 | 0 | 0 | 2 | 3.30 | 19369 | 79 | y |
| 38 | 12:17:15.27 | 12:41:57.3 | 15.6 | 0 | 1 | 64 | 374 | 3 | 3.44 | 17778 | 79 | y |
| 39 | 12:17:19.64 | 12:51:09.4 | 17.2 | 1 | 0 | 66 | 0 | 2 | 3.55 | 20555 | 144 | y |
| 40 | 12:17:20.57 | 11:57:05.4 | 16.7 | 0 | 1 | 68 | 0 | 3 | 1 | 7873 | 105 | y |
| 41 | 12:17:21.81 | 11:18:22.0 | 17.3 | 2 | 0 | 70 | 0 | 4 | 3.68 | 43962 | 136 | y |
| 42 | 12:17:25.56 | 12:12:58.9 | 17.6 | 1 | 0 | 74 | 0 | 2 | 3.12 | 19339 | 78 | y |
| 43 | 12:17:31.04 | 13:25:23.8 | 17.5 | 1 | 0 | 79 | 0 | 5 | 6.78 | 16248 | 52 | y |
| 44 | 12:17:42.95 | 13:41:42.3 | 17.6 | 1 | 0 | 85 | 0 | 4 | 2 | 24681 | 105 | y |
| 45 | 12:17:44.01 | 10:56:24.3 | 17.3 | 2 | 0 | 87 | 0 | 5 | 3.99 | 20378 | 74 | y |
| 46 | 12:17:47.79 | 13:46:21.7 | 17.3 | 1 | 0 | 88 | 0 | - | - | - | - | - |
| 47 | 12:17:49.26 | 12:27:53.8 | 17.7 | 1 | 0 | 90 | 410 | - | 0 | 283 | 0 | (2) BCD |
| 48 | 12:17:51.19 | 12:51:22.2 | 17.3 | 1 | 1 | 95 | 0 | 1 | 2 | 7768 | 80 | y |
| 49 | 12:17:55.00 | 14:50:04.9 | 17.5 | 1 | 0 | 96 | 0 | 4 | 3 | 12388 | 39 | y |
| 50 | 12:17:55.28 | 13:51:21.2 | 17.9 | 2 | 0 | 97 | 0 | 4 | 4.00 | 19705 | 83 | y |
| 51 | 12:17:57.53 | 11:37:04.9 | 15.9 | 2 | 1 | 99 | 420 | 1 | 5.57 | 12831 | 60 | y |
| 52 | 12:18:00.11 | 12:40:08.4 | 17.2 | 1 | 1 | 101 | 0 | 1 | 3.06 | 8059 | 103 | y |
| 53 | 12:18:03.48 | 14:30:52.1 | 17.7 | 1 | 0 | 102 | 0 | - | - | - | - | - |
| 54 | 12:18:04.42 | 13:40:18.0 | 16.5 | 2 | 1 | 103 | 0 | 1 | 5.79 | 12923 | 57 | y |
| 55 | 12:18:07.91 | 14:09:59.0 | 17.4 | 1 | 0 | 105 | 428 | - | 0 | 792 | 0 | (3) BCD |
| 56 | 12:18:09.45 | 11:40:43.4 | 17.4 | 1 | 0 | 0 | 0 | 2 | 4 | 27909 | 32 | y |
| 57 | 12:18:14.31 | 10:47:20.0 | 17.0 | 2 | 0 | 110 | 0 | 2 | 5.10 | 20290 | 51 | y |
| 58 | 12:18:14.93 | 12:09:51.2 | 17.0 | 0 | 1 | 112 | 0 | 3 | 3 | 11711 | 23 | y |
| 59 | 12:18:21.99 | 11:26:20.5 | 16.2 | 0 | 1 | 114 | 443 | 1 | 3.54 | 20487 | 103 | y |
| 60 | 12:18:27.24 | 13:44:48.9 | 16.9 | 0 | 1 | 117 | 0 | 3 | 4.10 | 26380 | 65 | y |
| 61 | 12:18:32.23 | 11:54:29.6 | 16.9 | 1 | 1 | 123 | 0 | 1 | 4 | 20649 | 16 | y |
| 62 | 12:18:34.08 | 14:04:17.1 | 17.5 | 1 | 0 | 0 | 0 | 5 | 7.06 | 25245 | 70 | y |
| 63 | 12:18:47.67 | 15:29:31.7 | 17.5 | 1 | 0 | 133 | 0 | 2 | 1 | 25362 | 214 | ? |
| 64 | 12:18:49.50 | 15:25:16.2 | 17.4 | 1 | 0 | 135 | 0 | - | - | - | - | - |

**Table 9** – *continued* Combined sample of BCD candidates and other galaxies observed

| N | R.A. (B1950) | Dec. | $B_J$ | B | Y | VPC | VCC | Run | R | $v_{\rm helio}$ | $\sigma_v$ | comment |
|---|---|---|---|---|---|---|---|---|---|---|---|---|
| 65 | 12:18:54.04 | 12:02:05.7 | 16.7 | 0 | 1 | 139 | 0 | 1 | 5.55 | 19415 | 81 | y |
| 66 | 12:18:55.20 | 11:56:04.0 | 17.9 | 1 | 0 | 141 | 0 | 4 | 3 | 7525 | 27 | y |
| 67 | 12:18:58.48 | 12:47:45.3 | 17.3 | 1 | 1 | 145 | 0 | 3 | 2 | 17463 | 216 | y |
| 68 | 12:19:02.38 | 14:03:26.6 | 17.6 | 2 | 0 | 147 | 0 | 4 | 3.69 | 24519 | 59 | y |
| 69 | 12:19:06.50 | 10:37:27.0 | 17.5 | 2 | 0 | 0 | 0 | - | - | - | - | - |
| 70 | 12:19:07.11 | 15:40:31.7 | 17.3 | 2 | 0 | 0 | 0 | 5 | - | - | - | star |
| 71 | 12:19:09.20 | 12:53:26.6 | 17.6 | 1 | 0 | 151 | 0 | 5 | 6.14 | 17332 | 59 | y |
| 72 | 12:19:09.51 | 13:05:44.9 | 17.5 | 1 | 0 | 154 | 0 | 5 | 5.79 | 7832 | 67 | y |
| 73 | 12:19:11.40 | 14:01:54.5 | 17.0 | 0 | 1 | 156 | 0 | 3 | 4.24 | 24464 | 63 | y |
| 74 | 12:19:12.08 | 12:31:51.2 | 17.8 | 1 | 0 | 157 | 0 | 5 | 5.76 | 11643 | 74 | y |
| 75 | 12:19:12.96 | 10:52:22.3 | 15.3 | 0 | 1 | 159 | 500 | 3 | 4.37 | 7840 | 57 | y |
| 76 | 12:19:13.71 | 11:12:56.5 | 17.7 | 1 | 0 | 160 | 0 | 4 | 2 | 16120 | 58 | y |
| 77 | 12:19:15.99 | 13:50:23.2 | 17.1 | 1 | 1 | 163 | 0 | 1 | 6.79 | 19264 | 51 | y |
| 78 | 12:19:17.64 | 14:53:43.4 | 17.4 | 1 | 0 | 164 | 0 | - | - | - | - | - |
| 79 | 12:19:19.79 | 10:41:03.8 | 17.5 | 1 | 0 | 0 | 0 | 2 | 3.39 | 20644 | 99 | y |
| 80 | 12:19:20.49 | 13:58:09.5 | 17.2 | 2 | 0 | 167 | 0 | 2 | 4.29 | 25636 | 72 | y |
| 81 | 12:19:21.62 | 12:04:48.8 | 17.6 | 1 | 0 | 169 | 0 | 5 | 6.77 | 19259 | 56 | y |
| 82 | 12:19:23.54 | 13:07:22.6 | 17.2 | 2 | 0 | 0 | 0 | 1 | 3.90 | 12561 | 82 | y |
| 83 | 12:19:29.74 | 10:53:52.1 | 16.5 | 1 | 1 | 176 | 0 | 1a | 2 | 7663 | 35 | y |
| 84 | 12:19:33.34 | 12:10:30.5 | 16.8 | 1 | 1 | 180 | 0 | 1 | 3.86 | 20895 | 97 | y |
| 85 | 12:19:35.37 | 15:01:04.1 | 17.7 | 1 | 0 | 187 | 0 | - | - | - | - | - |
| 86 | 12:19:40.54 | 13:40:10.5 | 17.4 | 1 | 0 | 192 | 0 | 5 | 4.61 | 19280 | 86 | y |
| 87 | 12:19:42.93 | 14:20:59.2 | 17.7 | 1 | 0 | 195 | 0 | - | - | - | - | - |
| 88 | 12:19:44.10 | 12:12:31.3 | 17.4 | 1 | 0 | 197 | 0 | 2 | 2 | 27633 | 53 | y |
| 89 | 12:19:44.60 | 12:40:26.0 | 17.0 | 1 | 0 | 198 | 0 | 2 | 3 | 6437 | 59 | y |
| 90 | 12:19:51.05 | 13:44:15.0 | 17.0 | 1 | 0 | 206 | 0 | 2 | 3 | 12856 | 29 | y |
| 91 | 12:19:52.27 | 15:01:26.7 | 16.9 | 0 | 1 | 208 | 0 | 3 | 4.76 | 4137 | 57 | y |
| 92 | 12:19:58.60 | 13:23:09.7 | 18.4 | 1 | 0 | 213 | 0 | - | - | - | - | - |
| 93 | 12:20:03.76 | 13:59:38.6 | 17.2 | 1 | 1 | 219 | 0 | 1 | 3.57 | 12681 | 82 | y |
| 94 | 12:20:04.69 | 13:43:28.6 | 17.2 | 1 | 1 | 221 | 0 | 1 | 4 | 12755 | 49 | y |
| 95 | 12:20:12.71 | 12:34:15.7 | 15.9 | 0 | 1 | 226 | 580 | 3 | 3.55 | 27499 | 110 | y |
| 96 | 12:20:14.79 | 12:23:58.6 | 17.1 | 1 | 1 | 228 | 0 | 1 | 5.89 | 24446 | 55 | y |
| 97 | 12:20:15.22 | 12:24:34.6 | 17.8 | 1 | 0 | 229 | 0 | - | - | - | - | - |
| 98 | 12:20:17.12 | 12:51:27.2 | 17.0 | 2 | 1 | 232 | 0 | 1 | 6.59 | 17393 | 52 | y |
| 99 | 12:20:22.61 | 12:50:37.5 | 16.7 | 0 | 1 | 236 | 0 | 3 | 2 | 7596 | 53 | y |
| 100 | 12:20:23.83 | 12:34:12.5 | 17.5 | 1 | 0 | 0 | 0 | - | - | - | - | - |
| 101 | 12:20:24.79 | 12:30:19.7 | 17.6 | 1 | 0 | 241 | 0 | 4 | 3.86 | 24434 | 77 | y |
| 102 | 12:20:25.61 | 13:49:23.3 | 16.5 | 0 | 1 | 244 | 0 | 1 | 3 | 7632 | 54 | y |
| 103 | 12:20:25.64 | 10:45:13.5 | 16.3 | 0 | 1 | 243 | 0 | 3 | 7.17 | 7692 | 61 | y |
| 104 | 12:20:28.65 | 10:51:59.3 | 17.8 | 1 | 0 | 247 | 0 | 4 | 4.05 | 7001 | 51 | y |
| 105 | 12:20:31.36 | 14:03:46.8 | 17.8 | 1 | 0 | 249 | 0 | - | - | - | - | - |
| 106 | 12:20:34.16 | 12:35:32.0 | 17.1 | 1 | 1 | 251 | 0 | 1 | 1 | 20856 | 80 | y |
| 107 | 12:20:34.67 | 10:38:20.8 | 16.8 | 1 | 0 | 0 | 0 | 2 | 4 | 20560 | 73 | y |
| 108 | 12:20:38.23 | 14:37:24.5 | 17.5 | 1 | 0 | 257 | 0 | 4 | 1 | 13000 | 86 | y |
| 109 | 12:20:41.08 | 14:28:55.9 | 17.5 | 1 | 0 | 262 | 0 | 5 | 9.40 | 12675 | 47 | y |
| 110 | 12:20:41.46 | 14:42:51.1 | 17.4 | 1 | 1 | 264 | 0 | 3 | 4 | 13075 | 23 | y |
| 111 | 12:20:42.26 | 10:47:17.5 | 17.3 | 1 | 0 | 265 | 0 | 4 | 3.44 | 7217 | 71 | y |
| 112 | 12:20:43.84 | 13:16:21.9 | 17.7 | 2 | 0 | 268 | 0 | 2 | 3.30 | 26018 | 145 | y |
| 113 | 12:20:44.83 | 13:19:43.3 | 16.5 | 0 | 1 | 272 | 0 | 3 | 1 | 24925 | 99 | y |
| 114 | 12:20:45.98 | 12:11:28.1 | 17.4 | 1 | 0 | 273 | 0 | 2 | 1 | 25132 | 92 | y |
| 115 | 12:20:46.25 | 12:13:37.1 | 17.4 | 1 | 0 | 274 | 0 | 4 | 5.28 | 19570 | 55 | y |
| 116 | 12:20:47.40 | 14:34:50.5 | 16.2 | 0 | 1 | 275 | 0 | 1 | 3.64 | 12426 | 87 | y |
| 117 | 12:20:49.18 | 11:51:16.1 | 17.2 | 1 | 1 | 277 | 0 | 1 | 1 | 19769 | 92 | y |
| 118 | 12:20:49.96 | 15:58:53.8 | 17.2 | 1 | 0 | 0 | 0 | - | - | - | - | - |
| 119 | 12:20:51.78 | 15:26:55.8 | 16.2 | 1 | 0 | 283 | 0 | 5 | 8.81 | 12550 | 54 | y |
| 120 | 12:20:51.91 | 13:13:25.0 | 16.6 | 0 | 1 | 282 | 0 | 1 | 4.51 | 7570 | 67 | y |
| 121 | 12:20:58.90 | 10:57:59.9 | 17.1 | 1 | 0 | 288 | 0 | 2 | 4 | 7352 | 18 | y |
| 122 | 12:21:02.07 | 13:15:05.8 | 17.5 | 1 | 0 | 290 | 0 | 5 | 4.60 | 24901 | 82 | y |
| 123 | 12:21:02.39 | 13:10:27.7 | 17.2 | 0 | 1 | 292 | 0 | 3 | 3.62 | 24959 | 69 | y |
| 124 | 12:21:05.16 | 13:28:19.4 | 17.5 | 1 | 0 | 295 | 0 | 4 | 4.03 | 12661 | 64 | y |
| 125 | 12:21:13.19 | 15:21:18.1 | 17.2 | 1 | 1 | 304 | 0 | 3 | 2 | 12737 | 45 | y |
| 126 | 12:21:16.88 | 14:24:57.4 | 17.5 | 1 | 0 | 309 | 0 | 2 | 3 | 12731 | 44 | y |
| 127 | 12:21:27.24 | 11:36:44.3 | 16.9 | 1 | 1 | 322 | 0 | 1 | 5.18 | 19655 | 63 | y |
| 128 | 12:21:30.36 | 11:07:31.6 | 17.3 | 2 | 0 | 326 | 0 | 4 | 2 | 8411 | 78 | y |

**Table 9** – *continued* Combined sample of BCD candidates and other galaxies observed

| N | R.A. (B1950) | Dec. | $B_J$ | B | Y | VPC | VCC | Run | R | $v_{\rm helio}$ | $\sigma_v$ | comment |
|---|---|---|---|---|---|---|---|---|---|---|---|---|
| 129 | 12:21:32.87 | 15:14:11.5 | 17.4 | 1 | 1 | 330 | 0 | 1 | 3 | 7138 | 41 | y |
| 130 | 12:21:32.88 | 15:09:46.7 | 18.3 | 1 | 0 | 333 | 0 | 4 | 3.99 | 26088 | 93 | y |
| 131 | 12:21:33.24 | 12:00:39.1 | 17.5 | 1 | 0 | 331 | 0 | 2 | 1 | 20939 | 58 | y |
| 132 | 12:21:47.01 | 10:43:23.5 | 16.5 | 0 | 1 | 341 | 0 | 3 | 1 | 18044 | 72 | y |
| 133 | 12:21:56.05 | 14:12:34.4 | 17.7 | 2 | 0 | 343 | 0 | - | - | - | - | - |
| 134 | 12:21:56.26 | 13:39:43.4 | 17.2 | 1 | 0 | 0 | 0 | 5 | 12.5 | 5980 | 31 | y |
| 135 | 12:22:00.63 | 12:58:55.6 | 16.9 | 2 | 1 | 350 | 0 | 1 | 4.98 | 7555 | 60 | y |
| 136 | 12:22:02.33 | 11:10:07.3 | 17.5 | 1 | 0 | 353 | 0 | 2 | 5 | 7560 | 16 | y |
| 137 | 12:22:02.79 | 14:17:16.9 | 17.6 | 2 | 0 | 354 | 0 | 4 | 3.73 | 24794 | 83 | y |
| 138 | 12:22:05.08 | 11:06:56.6 | 16.0 | 0 | 1 | 356 | 736 | 3 | 1 | 7661 | 176 | y |
| 139 | 12:22:06.72 | 10:52:30.5 | 17.0 | 1 | 1 | 357 | 0 | 1 | 4.34 | 7185 | 65 | y |
| 140 | 12:22:13.41 | 14:38:50.6 | 17.0 | 1 | 1 | 360 | 0 | 1 | 3 | 11346 | 51 | y |
| 141 | 12:22:16.07 | 12:17:43.1 | 16.5 | 0 | 1 | 365 | 0 | 3 | 3.87 | 17298 | 50 | y |
| 142 | 12:22:16.97 | 12:46:12.9 | 17.7 | 1 | 0 | 367 | 0 | - | - | - | - | - |
| 143 | 12:22:18.48 | 12:26:04.6 | 17.0 | 1 | 0 | 368 | 0 | 5 | 4.74 | 19435 | 92 | y |
| 144 | 12:22:19.93 | 12:32:11.5 | 17.6 | 1 | 0 | 371 | 0 | 4 | 4.35 | 24995 | 86 | y |
| 145 | 12:22:20.93 | 14:17:51.7 | 17.6 | 2 | 0 | 373 | 0 | 4 | 3.44 | 25067 | 129 | y |
| 146 | 12:22:22.76 | 12:23:21.3 | 17.5 | 2 | 0 | 374 | 0 | 4 | 4.87 | 19667 | 70 | y |
| 147 | 12:22:23.25 | 12:22:34.7 | 17.0 | 2 | 1 | 376 | 0 | 1 | 6.59 | 19245 | 69 | y |
| 148 | 12:22:27.49 | 12:16:13.1 | 17.4 | 2 | 0 | 0 | 0 | 2 | 3.79 | 30319 | 86 | y |
| 149 | 12:22:31.08 | 15:06:33.8 | 17.4 | 1 | 0 | 383 | 0 | 5 | 7.47 | 21530 | 59 | y |
| 150 | 12:22:36.38 | 13:43:39.8 | 16.8 | 1 | 1 | 388 | 0 | 1 | 3 | 11657 | 58 | y |
| 151 | 12:22:38.49 | 12:09:51.6 | 17.6 | 1 | 0 | 391 | 0 | 5 | 3.52 | 17372 | 92 | y |
| 152 | 12:22:40.50 | 14:18:58.1 | 16.0 | 0 | 1 | 393 | 0 | 1 | 4.48 | 12781 | 75 | y |
| 153 | 12:22:45.53 | 14:26:57.7 | 16.1 | 0 | 1 | 399 | 790 | 3 | 4.77 | 573 | 54 | y |
| 154 | 12:22:46.92 | 15:02:24.0 | 17.0 | 1 | 1 | 402 | 0 | 3 | 3.09 | 13201 | 79 | y |
| 155 | 12:22:51.42 | 14:29:36.9 | 17.7 | 1 | 0 | 411 | 0 | 5 | 6.08 | 24200 | 68 | y |
| 156 | 12:23:37.04 | 11:08:50.5 | 17.5 | 1 | 0 | 453 | 0 | 5 | 8.25 | 11818 | 50 | y |
| 157 | 12:23:42.46 | 16:08:29.7 | 17.7 | 1 | 0 | 0 | 0 | 4 | 3.34 | 24071 | 128 | ? |
| 158 | 12:23:47.96 | 12:03:07.8 | 17.4 | 1 | 0 | 459 | 0 | 2 | 4.61 | 16559 | 52 | y |
| 159 | 12:23:54.77 | 13:44:58.1 | 17.0 | 0 | 1 | 466 | 0 | 3 | 2 | 13091 | 62 | y |
| 160 | 12:24:01.63 | 14:37:58.7 | 16.8 | 0 | 1 | 476 | 0 | 3 | 4.25 | 23936 | 54 | y |
| 161 | 12:24:03.75 | 11:07:18.3 | 16.8 | 2 | 1 | 478 | 0 | 1 | 4.97 | 19749 | 101 | y |
| 162 | 12:24:04.75 | 14:38:21.9 | 17.5 | 2 | 0 | 480 | 0 | 4 | 4.07 | 24377 | 75 | y |
| 163 | 12:24:10.94 | 11:02:57.1 | 16.6 | 0 | 1 | 490 | 0 | 3 | 3.11 | 20103 | 90 | y |
| 164 | 12:24:12.11 | 11:11:41.3 | 16.4 | 1 | 0 | 0 | 0 | 1 | 2 | 7587 | 38 | y |
| 165 | 12:24:12.54 | 11:30:15.5 | 17.7 | 2 | 0 | 493 | 0 | 4 | 4.82 | 30834 | 80 | y |
| 166 | 12:24:13.90 | 12:31:22.8 | 17.6 | 1 | 0 | 495 | 0 | 2 | 3.54 | 25336 | 76 | y |
| 167 | 12:24:16.83 | 14:58:14.2 | 17.2 | 2 | 1 | 499 | 0 | 1 | 6.46 | 20011 | 49 | y |
| 168 | 12:24:22.77 | 13:50:33.8 | 16.3 | 0 | 1 | 508 | 953 | 1 | 3.46 | -503 | 78 | y |
| 169 | 12:24:32.16 | 10:55:20.2 | 17.9 | 1 | 0 | 515 | 0 | 5 | 3.18 | 40117 | 116 | y |
| 170 | 12:24:43.30 | 11:10:52.6 | 17.2 | 2 | 0 | 520 | 0 | - | - | - | - | - |
| 171 | 12:25:09.98 | 12:21:57.8 | 16.4 | 0 | 1 | 545 | 1035 | 3 | 4.19 | 182 | 89 | y |
| 172 | 12:25:14.86 | 11:27:25.7 | 17.7 | 2 | 0 | 552 | 0 | 4 | 3.89 | 17858 | 70 | y |
| 173 | 12:25:16.28 | 10:57:19.7 | 17.1 | 2 | 0 | 555 | 0 | - | - | - | - | - |
| 174 | 12:25:19.38 | 14:50:08.4 | 17.1 | 0 | 1 | 557 | 0 | 3 | 5.00 | 21401 | 55 | y |
| 175 | 12:25:22.98 | 13:42:35.4 | 17.4 | 1 | 0 | 562 | 0 | - | - | - | - | - |
| 176 | 12:25:34.97 | 12:13:51.0 | 17.3 | 1 | 0 | 0 | 0 | - | - | - | - | - |
| 177 | 12:25:36.58 | 15:00:05.3 | 17.1 | 1 | 1 | 576 | 0 | 1 | 3 | 21432 | 61 | y |
| 178 | 12:25:38.89 | 13:46:50.1 | 17.0 | 2 | 1 | 579 | 0 | 1 | 2.97 | 25422 | 95 | y |
| 179 | 12:25:40.94 | 12:21:25.2 | 17.3 | 2 | 0 | 581 | 0 | 4 | 4.30 | 26997 | 93 | y |
| 180 | 12:25:46.46 | 15:44:45.9 | 17.3 | 2 | 0 | 0 | 0 | 4 | 3.95 | 17515 | 86 | y |
| 181 | 12:25:48.83 | 15:20:07.4 | 17.2 | 1 | 1 | 595 | 0 | 1 | 5 | 17419 | 22 | y |
| 182 | 12:25:49.00 | 12:12:40.6 | 17.8 | 1 | 0 | 594 | 0 | - | - | - | - | - |
| 183 | 12:25:50.72 | 13:36:13.3 | 17.8 | 1 | 0 | 596 | 0 | 5 | 10.6 | 17048 | 37 | y |
| 184 | 12:26:01.25 | 12:14:25.2 | 17.2 | 2 | 1 | 603 | 0 | 1 | 8.54 | 26748 | 48 | y |
| 185 | 12:26:03.26 | 12:16:27.0 | 16.6 | 0 | 1 | 605 | 0 | 3 | 1 | 17064 | 121 | y |
| 186 | 12:26:10.49 | 10:57:43.4 | 17.6 | 1 | 0 | 611 | 0 | - | - | - | - | - |
| 187 | 12:26:21.38 | 15:51:34.0 | 17.4 | 1 | 0 | 0 | 0 | 4 | 1 | 21486 | 78 | y |
| 188 | 12:26:24.60 | 10:47:34.2 | 17.6 | 1 | 0 | 0 | 0 | 4 | 1 | 19344 | 227 | y |
| 189 | 12:26:26.27 | 12:56:11.1 | 16.6 | 0 | 1 | 624 | 1148 | 3 | 6.00 | 1443 | 44 | y |
| 190 | 12:26:31.19 | 11:05:08.2 | 17.6 | 2 | 0 | 630 | 0 | 4 | 3.42 | 25846 | 110 | y |
| 191 | 12:26:31.30 | 10:41:31.3 | 17.4 | 1 | 0 | 0 | 0 | 4 | 5.41 | 19021 | 93 | y |
| 192 | 12:26:33.54 | 11:47:55.6 | 17.6 | 1 | 0 | 635 | 0 | - | - | - | - | - |

**Table 9** – *continued* Combined sample of BCD candidates and other galaxies observed

| N | R.A. (B1950) | Dec. | $B_J$ | B | Y | VPC | VCC | Run | R | $v_{\rm helio}$ | $\sigma_v$ | comment |
|---|---|---|---|---|---|---|---|---|---|---|---|---|
| 193 | 12:26:37.91 | 14:47:59.8 | 17.5 | 2 | 0 | 639 | 0 | 5 | 2 | 6188 | 100 | y |
| 194 | 12:26:38.96 | 14:35:37.7 | 17.3 | 1 | 0 | 640 | 0 | 2 | 3 | 12620 | 25 | y |
| 195 | 12:26:40.97 | 12:23:13.0 | 17.6 | 2 | 0 | 641 | 0 | 4 | 4.90 | 26792 | 54 | y |
| 196 | 12:26:42.98 | 13:15:15.7 | 16.4 | 0 | 1 | 642 | 1173 | 3 | 3.22 | 2468 | 68 | y |
| 197 | 12:26:43.70 | 10:41:21.8 | 17.2 | 2 | 0 | 0 | 0 | 5 | - | - | - | star |
| 198 | 12:26:46.01 | 12:00:39.3 | 17.5 | 1 | 0 | 646 | 0 | 4 | 4.30 | 25616 | 84 | y |
| 199 | 12:26:49.53 | 15:03:56.0 | 16.0 | 0 | 1 | 650 | 0 | 3 | 3.65 | 17429 | 63 | y |
| 200 | 12:26:51.98 | 12:03:58.0 | 17.1 | 1 | 0 | 654 | 0 | - | - | - | - | - |
| 201 | 12:26:52.01 | 15:02:06.3 | 17.0 | 0 | 1 | 656 | 0 | 1 | 4.03 | 17114 | 83 | y |
| 202 | 12:26:52.99 | 12:58:06.0 | 17.4 | 1 | 0 | 657 | 0 | 4 | 5.65 | 28000 | 55 | y |
| 203 | 12:26:53.70 | 13:34:34.9 | 16.8 | 0 | 1 | 658 | 0 | 3 | 3.11 | 25027 | 94 | y |
| 204 | 12:26:54.73 | 14:31:09.3 | 17.4 | 1 | 0 | 0 | 0 | 2 | 1 | 21379 | 33 | y |
| 205 | 12:26:55.83 | 14:06:24.4 | 16.7 | 0 | 1 | 663 | 0 | 3 | 1 | 19241 | 197 | y |
| 206 | 12:27:06.86 | 11:41:21.4 | 17.4 | 2 | 0 | 674 | 0 | 2 | 4 | 18430 | 40 | y |
| 207 | 12:27:08.25 | 12:34:19.4 | 17.6 | 1 | 0 | 0 | 0 | 4 | 4 | 26076 | 35 | y |
| 208 | 12:27:09.18 | 11:56:25.3 | 17.7 | 2 | 0 | 679 | 0 | 5 | 2 | 22266 | 106 | ? |
| 209 | 12:27:09.30 | 12:06:56.5 | 17.4 | 1 | 0 | 680 | 0 | - | - | - | - | - |
| 210 | 12:27:09.60 | 12:03:53.6 | 17.5 | 1 | 0 | 681 | 0 | 4 | 4.85 | 25384 | 74 | y |
| 211 | 12:27:10.78 | 11:01:58.4 | 16.5 | 0 | 1 | 682 | 1217 | 3 | 3.75 | 25662 | 74 | ? |
| 212 | 12:27:13.52 | 12:36:17.3 | 17.5 | 1 | 0 | 0 | 0 | - | - | - | - | - |
| 213 | 12:27:14.54 | 14:31:32.3 | 17.7 | 1 | 0 | 686 | 0 | - | - | - | - | - |
| 214 | 12:27:17.96 | 12:18:56.9 | 17.1 | 1 | 1 | 688 | 0 | 1 | 4.46 | 16200 | 70 | y |
| 215 | 12:27:18.18 | 12:05:10.9 | 17.9 | 1 | 0 | 691 | 0 | 5 | 3.75 | 26334 | 93 | y |
| 216 | 12:27:19.05 | 13:31:40.3 | 17.7 | 1 | 0 | 692 | 0 | 4 | 2 | 24839 | 50 | y |
| 217 | 12:27:19.49 | 14:08:38.1 | 16.1 | 0 | 1 | 694 | 1237 | 1 | 3.10 | -336 | 90 | y |
| 218 | 12:27:20.17 | 11:48:04.8 | 16.9 | 0 | 1 | 696 | 0 | 1 | 5.34 | 17508 | 61 | y |
| 219 | 12:27:20.34 | 12:03:23.0 | 15.6 | 0 | 1 | 697 | 0 | 3 | 3.68 | 25026 | 111 | y |
| 220 | 12:27:23.04 | 14:57:52.9 | 16.0 | 0 | 1 | 703 | 0 | 3 | 3.16 | 23973 | 86 | y |
| 221 | 12:27:24.23 | 10:53:28.7 | 14.7 | 0 | 1 | 704 | 1243 | 1 | 5.52 | 7338 | 65 | y |
| 222 | 12:27:25.07 | 11:11:27.6 | 17.4 | 2 | 0 | 705 | 0 | 2 | 3.71 | 7668 | 64 | y |
| 223 | 12:27:29.79 | 15:08:59.6 | 16.9 | 1 | 1 | 709 | 0 | 1 | 1 | 17597 | 63 | y |
| 224 | 12:27:34.02 | 11:06:23.6 | 17.5 | 2 | 0 | 717 | 0 | 4 | 3.63 | 25945 | 83 | y |
| 225 | 12:27:34.06 | 11:30:44.7 | 17.5 | 1 | 0 | 718 | 0 | 2 | 2 | 17694 | 38 | y |
| 226 | 12:27:39.71 | 12:23:04.2 | 17.1 | 1 | 0 | 0 | 0 | 5 | 4.12 | 25254 | 159 | y |
| 227 | 12:27:40.96 | 13:43:53.0 | 17.4 | 2 | 0 | 726 | 0 | 2 | 3.64 | 25215 | 70 | y |
| 228 | 12:27:41.35 | 11:19:37.5 | 17.7 | 1 | 0 | 728 | 0 | - | - | - | - | - |
| 229 | 12:27:43.33 | 12:40:22.9 | 17.3 | 2 | 0 | 733 | 0 | 4 | 4.90 | 25847 | 81 | y |
| 230 | 12:27:43.76 | 12:02:32.6 | 17.4 | 1 | 0 | 734 | 0 | 2 | 4.18 | 26613 | 81 | y |
| 231 | 12:27:49.70 | 12:01:39.4 | 17.5 | 1 | 0 | 744 | 0 | 4 | 3.46 | 26651 | 85 | y |
| 232 | 12:27:50.84 | 11:08:43.3 | 16.8 | 1 | 0 | 0 | 0 | - | - | - | - | - |
| 233 | 12:27:51.80 | 11:17:24.4 | 17.9 | 1 | 0 | 745 | 0 | 4 | 1 | 20360 | 206 | y |
| 234 | 12:27:53.28 | 13:44:17.1 | 17.6 | 2 | 0 | 748 | 0 | 4 | 4.01 | 24633 | 88 | y |
| 235 | 12:27:54.18 | 10:47:32.1 | 17.4 | 1 | 0 | 749 | 0 | 2 | 3 | 7555 | 41 | y |
| 236 | 12:28:02.64 | 13:01:48.8 | 16.9 | 1 | 1 | 0 | 0 | 1 | 1 | 27457 | 114 | y |
| 237 | 12:28:08.35 | 14:20:15.3 | 17.1 | 1 | 1 | 759 | 0 | 1 | 1 | 21265 | 97 | y |
| 238 | 12:28:13.01 | 12:38:33.2 | 17.2 | 1 | 1 | 0 | 0 | 1 | 4.20 | 25383 | 75 | y |
| 239 | 12:28:16.59 | 12:19:15.8 | 17.8 | 1 | 0 | 768 | 1313 | - | 0 | 1254 | 0 | (4) BCD |
| 240 | 12:28:18.23 | 14:54:37.3 | 16.7 | 1 | 0 | 772 | 0 | 2 | 3 | 13473 | 23 | y |
| 241 | 12:28:24.34 | 11:54:11.6 | 17.0 | 0 | 1 | 776 | 0 | 3 | 4.88 | 25202 | 58 | y |
| 242 | 12:28:24.51 | 12:08:05.1 | 17.7 | 1 | 0 | 777 | 0 | - | - | - | - | - |
| 243 | 12:28:25.75 | 11:04:44.6 | 17.2 | 2 | 1 | 779 | 0 | 1 | 5.37 | 14659 | 63 | y |
| 244 | 12:28:29.14 | 10:45:29.1 | 17.0 | 1 | 0 | 0 | 0 | - | - | - | - | - |
| 245 | 12:28:39.08 | 10:55:23.2 | 17.5 | 1 | 0 | 794 | 0 | 2 | 3 | 25810 | 72 | y |
| 246 | 12:28:45.23 | 11:53:05.0 | 17.5 | 2 | 0 | 804 | 0 | 4 | 3.81 | 25387 | 63 | y |
| 247 | 12:28:45.81 | 10:57:20.8 | 16.8 | 0 | 1 | 805 | 0 | 3 | 4 | 27632 | 57 | y |
| 248 | 12:28:48.40 | 14:28:17.1 | 17.5 | 1 | 0 | 809 | 0 | - | - | - | - | - |
| 249 | 12:28:49.09 | 15:13:30.8 | 17.5 | 1 | 0 | 0 | 0 | - | - | - | - | - |
| 250 | 12:28:54.85 | 13:11:32.7 | 17.3 | 2 | 0 | 0 | 0 | 2 | ** | 28750 | ** | str+gal |
| 251 | 12:29:06.40 | 10:59:45.6 | 17.5 | 2 | 0 | 825 | 0 | 4 | 4.34 | 25685 | 83 | y |
| 252 | 12:29:08.23 | 15:15:38.6 | 17.3 | 2 | 1 | 830 | 0 | 1 | 4.13 | 21644 | 120 | y |
| 253 | 12:29:11.87 | 14:01:20.7 | 16.8 | 1 | 0 | 0 | 0 | - | - | - | - | - |
| 254 | 12:29:13.53 | 11:02:28.7 | 17.6 | 1 | 0 | 832 | 0 | - | - | - | - | - |
| 255 | 12:29:20.61 | 15:05:03.8 | 17.3 | 2 | 0 | 0 | 0 | - | - | - | - | - |
| 256 | 12:29:28.00 | 13:21:32.6 | 17.4 | 1 | 0 | 0 | 1403 | 1a | - | - | - | str+gal |

**Table 9** – *continued* Combined sample of BCD candidates and other galaxies observed

| N | R.A. (B1950) | Dec. | $B_J$ | B | Y | VPC | VCC | Run | R | $v_{\mathrm{helio}}$ | $\sigma_v$ | comment |
|---|---|---|---|---|---|---|---|---|---|---|---|---|
| 257 | 12:29:33.01 | 14:13:55.1 | 17.4 | 1 | 0 | 845 | 0 | 2 | 6 | 19350 | 18 | y |
| 258 | 12:29:36.02 | 11:49:41.9 | 17.4 | 2 | 0 | 851 | 0 | 2 | 6.63 | 25878 | 50 | y |
| 259 | 12:29:46.33 | 11:32:12.0 | 17.3 | 2 | 1 | 860 | 0 | 1 | 5.30 | 12208 | 69 | y |
| 260 | 12:29:46.66 | 12:36:25.1 | 17.5 | 1 | 0 | 861 | 0 | 4 | 1 | 27705 | 58 | y |
| 261 | 12:29:55.97 | 11:44:42.3 | 17.5 | 1 | 0 | 866 | 0 | 2 | 3.56 | 21404 | 85 | y |
| 262 | 12:29:57.18 | 11:39:00.7 | 17.6 | 1 | 0 | 867 | 0 | 5 | 7.31 | 7513 | 49 | y |
| 263 | 12:29:59.93 | 11:28:54.6 | 17.3 | 2 | 0 | 869 | 0 | 2 | 4.77 | 25893 | 55 | y |
| 264 | 12:30:00.46 | 14:00:21.6 | 17.0 | 1 | 0 | 871 | 0 | 5 | 18.52 | 16640 | 24 | y |
| 265 | 12:30:02.64 | 14:51:20.9 | 17.2 | 0 | 1 | 873 | 0 | 3 | 4 | 7211 | 36 | y |
| 266 | 12:30:21.32 | 11:17:45.4 | 17.3 | 2 | 0 | 886 | 0 | 2 | 4.20 | 19927 | 69 | y |
| 267 | 12:30:27.04 | 12:44:01.4 | 17.5 | 1 | 0 | 888 | 0 | 2 | 1 | 25810 | 276 | y |
| 268 | 12:30:32.76 | 15:32:16.2 | 17.2 | 2 | 0 | 892 | 0 | 4 | 4.17 | 34024 | 103 | y |
| 269 | 12:30:37.27 | 12:27:55.5 | 17.4 | 2 | 0 | 896 | 0 | 5 | 3.80 | 29175 | 111 | y |
| 270 | 12:30:42.39 | 13:08:00.1 | 15.3 | 0 | 1 | 899 | 1491 | 3 | 3.79 | 1811 | 68 | y |
| 271 | 12:30:45.84 | 11:55:16.3 | 17.5 | 1 | 0 | 0 | 0 | - | - | - | - | - |
| 272 | 12:30:48.13 | 13:07:44.1 | 16.0 | 1 | 0 | 0 | 1499 | - | 0 | -575 | 0 | (5) |
| 273 | 12:30:48.86 | 12:39:12.4 | 17.1 | 2 | 1 | 902 | 0 | 1 | 10.02 | 27562 | 37 | y |
| 274 | 12:30:49.50 | 13:30:03.6 | 16.8 | 0 | 1 | 903 | 0 | 3 | 2 | 7467 | 76 | y |
| 275 | 12:31:00.49 | 11:16:16.9 | 17.1 | 1 | 1 | 908 | 0 | 1 | 1 | 20630 | 73 | y |
| 276 | 12:31:06.64 | 12:18:37.0 | 17.8 | 1 | 0 | 914 | 0 | - | - | - | - | - |
| 277 | 12:31:07.16 | 11:23:52.3 | 18.0 | 1 | 0 | 915 | 0 | 4 | 3 | 29731 | 53 | y |
| 278 | 12:31:08.39 | 14:53:58.7 | 17.5 | 1 | 0 | 916 | 0 | 2 | 3 | 25535 | 52 | y |
| 279 | 12:31:18.23 | 12:53:52.2 | 17.0 | 2 | 0 | 921 | 0 | 4 | 3.38 | 28032 | 86 | y |
| 280 | 12:31:20.14 | 13:35:53.5 | 15.6 | 0 | 1 | 923 | 1528 | 1 | 6.69 | 1623 | 49 | y |
| 281 | 12:31:20.17 | 12:53:34.8 | 16.0 | 1 | 1 | 922 | 0 | 3 | 6.78 | 28060 | 52 | y |
| 282 | 12:31:31.08 | 10:38:42.1 | 17.5 | 1 | 0 | 0 | 0 | - | - | - | - | - |
| 283 | 12:31:31.61 | 11:17:24.1 | 17.0 | 0 | 1 | 932 | 0 | 3 | ** | ** | ** | str+gal |
| 284 | 12:31:31.98 | 13:17:12.7 | 16.6 | 0 | 1 | 931 | 0 | 3 | 1 | 12954 | 62 | y |
| 285 | 12:31:32.40 | 10:48:45.1 | 17.6 | 1 | 0 | 934 | 0 | 4 | 2 | 11956 | 68 | y |
| 286 | 12:31:36.91 | 13:34:26.0 | 16.5 | 0 | 1 | 939 | 0 | 3 | 4 | 13417 | 45 | y |
| 287 | 12:31:38.61 | 15:25:54.3 | 17.4 | 1 | 0 | 0 | 0 | - | - | - | - | - |
| 288 | 12:31:38.79 | 13:35:08.1 | 17.7 | 1 | 0 | 941 | 0 | - | - | - | - | - |
| 289 | 12:31:40.48 | 12:05:12.0 | 17.1 | 1 | 1 | 945 | 1544 | 1 | 5.28 | 16355 | 59 | y BCD? |
| 290 | 12:31:43.23 | 11:20:51.3 | 15.4 | 0 | 1 | 947 | 1549 | 1 | 4.46 | 1366 | 73 | y |
| 291 | 12:31:51.63 | 12:20:22.5 | 17.8 | 1 | 0 | 951 | 0 | 5 | 3.49 | 25397 | 113 | ? |
| 292 | 12:32:13.96 | 14:49:57.4 | 16.8 | 0 | 1 | 972 | 0 | 3 | 5.11 | 13720 | 76 | y |
| 293 | 12:32:18.11 | 13:31:50.0 | 16.7 | 1 | 1 | 975 | 0 | 1 | 3 | 16798 | 28 | y |
| 294 | 12:32:19.93 | 15:15:09.6 | 16.1 | 0 | 1 | 976 | 0 | 3 | 4.14 | 13612 | 59 | y |
| 295 | 12:32:22.07 | 11:19:31.8 | 17.8 | 1 | 0 | 977 | 0 | 2 | 4 | 20710 | 25 | y |
| 296 | 12:32:23.60 | 15:26:35.7 | 17.6 | 2 | 0 | 0 | 0 | 2 | 3.51 | 24406 | 131 | y |
| 297 | 12:32:25.94 | 11:48:16.7 | 17.4 | 2 | 0 | 980 | 0 | 2 | 3.50 | 20122 | 69 | y |
| 298 | 12:32:32.62 | 16:03:20.7 | 17.1 | 2 | 0 | 0 | 0 | 1 | 7.21 | 13748 | 46 | y |
| 299 | 12:32:33.79 | 11:53:52.9 | 16.9 | 0 | 1 | 983 | 0 | 3 | 4.78 | 24386 | 77 | y |
| 300 | 12:32:34.77 | 13:03:44.5 | 17.5 | 1 | 0 | 984 | 0 | - | - | - | - | - |
| 301 | 12:32:43.85 | 15:37:05.4 | 17.5 | 1 | 0 | 0 | 0 | - | - | - | - | - |
| 302 | 12:32:44.21 | 12:45:42.5 | 18.2 | 1 | 0 | 989 | 0 | - | - | - | - | - |
| 303 | 12:32:53.64 | 15:11:32.4 | 17.2 | 1 | 0 | 994 | 0 | 4 | 4.95 | 19143 | 84 | y |
| 304 | 12:33:00.84 | 16:04:46.0 | 17.4 | 1 | 0 | 0 | 0 | 2 | 1 | 24514 | 42 | y |
| 305 | 12:33:03.41 | 10:39:16.4 | 17.4 | 1 | 0 | 0 | 0 | 2 | 3.75 | 9599 | 56 | y |
| 306 | 12:33:06.00 | 11:22:41.6 | 17.2 | 1 | 0 | 1009 | 0 | 4 | 4.87 | 28279 | 53 | y |
| 307 | 12:33:06.81 | 12:45:29.1 | 16.5 | 0 | 1 | 1011 | 0 | 3 | 2 | 12505 | 46 | y |
| 308 | 12:33:09.53 | 11:56:31.7 | 16.1 | 0 | 1 | 1013 | 1633 | 3 | 1 | 16252 | 37 | y |
| 309 | 12:33:14.53 | 11:56:58.3 | 17.2 | 1 | 1 | 1017 | 0 | 1 | 3 | 18725 | 29 | y |
| 310 | 12:33:21.62 | 15:38:53.0 | 17.5 | 1 | 0 | 0 | 0 | 4 | 2 | 16051 | 129 | y |
| 311 | 12:33:23.62 | 12:38:42.5 | 17.0 | 1 | 1 | 1024 | 0 | 1 | 5.84 | 13594 | 50 | y |
| 312 | 12:33:25.93 | 11:51:09.6 | 17.8 | 1 | 0 | 1027 | 0 | 5 | 8.29 | 20126 | 48 | y |
| 313 | 12:33:28.65 | 12:40:28.6 | 17.6 | 2 | 0 | 1029 | 0 | 4 | 3.76 | 12904 | 112 | y |
| 314 | 12:33:29.44 | 13:12:40.2 | 17.6 | 1 | 0 | 1030 | 0 | 4 | 4.88 | 28077 | 66 | y |
| 315 | 12:33:30.81 | 11:50:02.4 | 17.6 | 1 | 0 | 1031 | 0 | 2 | 3.42 | 19831 | 81 | y |
| 316 | 12:33:31.16 | 12:07:31.2 | 17.5 | 1 | 0 | 1032 | 0 | 5 | 3.00 | 28279 | 79 | ? |
| 317 | 12:33:31.98 | 12:49:55.1 | 17.1 | 1 | 1 | 1033 | 0 | 3 | 3.16 | 13530 | 77 | y |
| 318 | 12:33:51.42 | 13:52:39.9 | 15.8 | 0 | 1 | 1047 | 1660 | 1 | 1 | 9092 | 110 | y |
| 319 | 12:33:54.06 | 13:15:13.7 | 17.6 | 1 | 0 | 1048 | 0 | - | - | - | - | - |
| 320 | 12:33:55.59 | 12:02:03.0 | 16.7 | 1 | 1 | 1051 | 0 | 1 | 1 | 19815 | 87 | y |

**Table 9** – *continued* Combined sample of BCD candidates and other galaxies observed

| N | R.A. (B1950) | Dec. | $B_J$ | B | Y | VPC | VCC | Run | R | $v_{\rm helio}$ | $\sigma_v$ | comment |
|---|---|---|---|---|---|---|---|---|---|---|---|---|
| 321 | 12:33:57.63 | 12:52:52.8 | 17.5 | 1 | 0 | 1053 | 0 | 5 | 4.42 | 13100 | 70 | y |
| 322 | 12:34:04.17 | 14:58:08.5 | 17.7 | 1 | 0 | 1065 | 0 | - | - | - | - | - |
| 323 | 12:34:05.89 | 10:49:21.4 | 17.4 | 1 | 0 | 1068 | 0 | 5 | 3 | 21513 | 55 | y |
| 324 | 12:34:11.97 | 14:32:40.0 | 16.5 | 0 | 1 | 1072 | 0 | 3 | 2 | 13788 | 45 | y |
| 325 | 12:34:12.88 | 14:55:12.1 | 17.2 | 1 | 1 | 1074 | 0 | 1 | 2 | 13767 | 72 | y |
| 326 | 12:34:16.07 | 15:28:36.1 | 17.8 | 1 | 0 | 1078 | 0 | - | - | - | - | - |
| 327 | 12:34:21.42 | 11:40:47.5 | 17.3 | 1 | 0 | 1084 | 0 | 2 | 4 | 16425 | 20 | y |
| 328 | 12:34:25.35 | 10:42:18.0 | 17.0 | 1 | 0 | 0 | 0 | 1 | 3.79 | 7220 | 102 | y |
| 329 | 12:34:31.57 | 10:41:15.7 | 17.5 | 1 | 0 | 0 | 0 | 2 | 1 | 7779 | 83 | y |
| 330 | 12:34:33.88 | 15:32:01.9 | 16.8 | 0 | 1 | 1096 | 0 | 1 | 4.47 | 22855 | 64 | y |
| 331 | 12:34:35.58 | 15:42:38.9 | 17.5 | 1 | 0 | 0 | 0 | - | - | - | - | - |
| 332 | 12:34:36.98 | 14:40:56.4 | 17.1 | 1 | 1 | 1097 | 0 | 1 | 5.77 | 9202 | 49 | y |
| 333 | 12:34:37.42 | 15:24:48.1 | 17.5 | 1 | 0 | 1098 | 0 | 4 | 1 | 22124 | 118 | y |
| 334 | 12:34:37.43 | 15:42:11.0 | 17.6 | 2 | 0 | 0 | 0 | 5 | 3.25 | 20968 | 177 | y |
| 335 | 12:34:38.49 | 14:59:34.1 | 17.4 | 1 | 0 | 0 | 0 | 2 | 3.40 | 26189 | 116 | y |
| 336 | 12:34:40.05 | 15:42:32.2 | 17.0 | 1 | 0 | 0 | 0 | - | - | - | - | - |
| 337 | 12:34:46.06 | 14:33:17.7 | 17.2 | 1 | 1 | 1102 | 0 | 1 | 6 | 13883 | 26 | y |
| 338 | 12:34:48.48 | 11:14:48.5 | 16.8 | 1 | 1 | 1105 | 0 | 1 | 2 | 17937 | 85 | y |
| 339 | 12:34:55.05 | 15:21:35.4 | 17.5 | 2 | 0 | 1107 | 0 | 2 | 3.99 | 21589 | 68 | y |
| 340 | 12:34:56.19 | 13:52:59.8 | 17.1 | 0 | 1 | 1108 | 0 | 3 | 3.14 | 21296 | 90 | y |
| 341 | 12:34:57.63 | 10:50:40.5 | 16.9 | 1 | 0 | 1109 | 0 | 2 | 5 | 16158 | 12 | y |
| 342 | 12:35:07.07 | 14:05:47.3 | 17.4 | 1 | 0 | 1116 | 0 | 5 | 4.09 | 13701 | 106 | y |
| 343 | 12:35:10.55 | 11:41:31.9 | 17.6 | 1 | 0 | 1118 | 0 | - | - | - | - | - |
| 344 | 12:35:15.92 | 12:17:15.6 | 17.7 | 1 | 0 | 1121 | 0 | 4 | 2 | 24142 | 38 | y |
| 345 | 12:35:22.83 | 15:29:56.4 | 15.6 | 0 | 1 | 1124 | 0 | 3 | 5.03 | 21449 | 63 | y |
| 346 | 12:35:25.80 | 10:37:37.7 | 17.1 | 1 | 0 | 0 | 0 | 1 | 1 | 25481 | 150 | y |
| 347 | 12:35:32.26 | 10:43:38.3 | 16.9 | 1 | 0 | 0 | 0 | - | - | - | - | - |
| 348 | 12:35:35.30 | 15:39:44.0 | 17.5 | 1 | 0 | 0 | 0 | 5 | 4.70 | 20859 | 72 | y |
| 349 | 12:35:35.42 | 14:08:55.0 | 17.6 | 1 | 0 | 0 | 0 | 4 | 1 | 21423 | 80 | ? |
| 350 | 12:35:37.22 | 14:18:33.4 | 17.3 | 1 | 0 | 0 | 0 | 5 | 3 | 13685 | 38 | y |
| 351 | 12:35:44.48 | 11:36:28.8 | 17.4 | 1 | 0 | 0 | 0 | - | - | - | - | - |
| 352 | 12:36:03.72 | 14:37:36.7 | 16.0 | 1 | 0 | 0 | 1765 | - | 0 | 9171 | 0 | (6) |
| 353 | 12:36:08.03 | 15:04:48.2 | 17.5 | 1 | 0 | 0 | 0 | - | - | - | - | - |
| 354 | 12:36:09.72 | 14:00:30.8 | 16.8 | 1 | 0 | 0 | 0 | 1 | 6.21 | 13846 | 58 | y |
| 355 | 12:36:20.34 | 13:50:08.4 | 17.4 | 1 | 0 | 0 | 0 | 5 | 2 | 21578 | 86 | y |
| 356 | 12:36:24.33 | 15:17:23.9 | 17.3 | 1 | 0 | 0 | 0 | 5 | 3.73 | 21235 | 109 | y |
| 357 | 12:36:26.54 | 11:24:17.4 | 17.0 | 1 | 0 | 0 | 0 | - | - | - | - | - |
| 358 | 12:36:29.33 | 15:32:39.6 | 17.4 | 2 | 0 | 0 | 0 | 2 | 4.22 | 21336 | 74 | y |
| 359 | 12:36:33.74 | 14:02:00.4 | 17.4 | 2 | 0 | 0 | 0 | 2 | 4.46 | 13686 | 67 | y |
| 360 | 12:36:39.00 | 13:44:47.0 | 17.6 | 1 | 0 | 0 | 0 | 4 | 1 | 23179 | 76 | y |
| 361 | 12:36:40.76 | 15:55:13.4 | 17.6 | 1 | 0 | 0 | 0 | 4 | 1 | 21883 | 57 | y |
| 362 | 12:36:44.29 | 14:21:52.1 | 16.9 | 1 | 0 | 0 | 0 | 1 | 5.45 | 22253 | 68 | y |
| 363 | 12:36:48.51 | 14:48:20.5 | 17.6 | 2 | 0 | 0 | 0 | 5 | 4.18 | 22213 | 79 | y |
| 364 | 12:36:50.63 | 12:28:11.9 | 17.6 | 1 | 0 | 0 | 1790 | 5 | 3.62 | 3604 | 159 | ? |
| 365 | 12:36:59.16 | 14:21:23.0 | 17.4 | 1 | 0 | 0 | 0 | 2 | 2 | 13483 | 72 | ? |
| 366 | 12:37:06.71 | 14:33:20.5 | 17.5 | 1 | 0 | 0 | 0 | - | - | - | - | - |
| 367 | 12:37:12.12 | 13:45:05.9 | 17.4 | 1 | 0 | 0 | 0 | 1a | 4.49 | 13920 | 71 | y |
| 368 | 12:37:12.87 | 14:31:09.2 | 17.2 | 1 | 0 | 0 | 0 | 2 | 3.55 | 9072 | 85 | y |
| 369 | 12:37:13.45 | 15:08:42.9 | 17.0 | 1 | 0 | 0 | 0 | 1 | 3 | 6486 | 31 | y |

Notes: The flags B (BCD, =1 if $B_J - R_C < 1.1$, =2 if redder) and Y (for the dE sample) indicate which samples the objects are in; VPC and VCC indicate entries in the respective Virgo reference catalogues; R is the number of emission lines fitted or the Tonry & Davis $R$ coefficient (see text); $v_{\rm helio}$ is the heliocentric corrected velocity ($cz$) and $\sigma_v$ the uncertainty, both in units of $\mathrm{km\,s^{-1}}$ ; the final comment indicates if the velocity identification is reliable ('y'), doubtful ('?') or based on high resolution data given in Table 5 ('star' or 'galaxy'). All the velocities are from our observations except (1), (5), (6) from Binggeli et al. (1985b) and (2), (3), (4) from Binggeli et al. (1993).